EXPERIMENTAL STUDY OF HEAT TRANSFER COEFFICIENT FOR NANOFLUID WITH INSERTED TAPE

NUR ASHIKIN BINTI USRI

Report submitted in partial fulfillment of the requirements
for the award of the degree of
Bachelor of Mechanical Engineering

Faculty of Mechanical Engineering
UNIVERSITI MALAYSIA PAHANG

DECEMBER 2010

SUPERVISOR'S DECLARATION

I hereby declare that I have checked this project and in my opinion, this project is adequate in terms of scope and quality for the award of the degree of Bachelor of Mechanical Engineering.

Signature
Name of Supervisor: WAN AZMI BIN WAN HAMZAH
Position: LECTURER
Date:

STUDENT'S DECLARATION

I hereby declare that the work in this thesis is my own except for quotations and summaries which have been duly acknowledged. The thesis has not been accepted for any degree and is not concurrently submitted for award of other degree.

Signature
Name: NUR ASHIKIN BINTI USRI
ID Number: MA07084
Date:

A small gift to my beloved parents for their love, patience and support within my whole life

ACKNOWLEDGEMENTS

With the name of ALLAH, the Most Merciful and the Most Beneficial. First and foremost, many praises for ALLAH and whole-heart grateful to the Great Creator as I have finished my final year research.

Starting with deepest thank you to my supervisor who is also my advisor, DMr. Wan Azmi Wan Hamzah, for giving me the opportunity to work with him in order to complete my Final Year Project 1. I am particularly thankful for the great confidence he had in me, for his support, enthusiasm and his guidance.

My thanks also go to my colleagues who always brainstorming additional new ideas and suggestions. Last but not least, I am grateful to my beloved Mother, Pn Hjh Mashita Binti Musa, my encouraged Father, En. Hj Usri Bin Salleh, my elder sister, Nur Azah Binti Usri, my younger sister, Nur Aqilah Binti Usri and my youngest brother, Mohammed Nur Arif Bin Usri for their love and never-ending encouragements in order to achieve my dreams. May ALLAH bless these people always.

Thank you all.

ABSTRACT

This thesis deals with a study of heat transfer coefficient for nanofluid with inserted tape. Research and development for enhancement heat transfer using nanofluid shows positive reaction for increasing the rate of convection heat transfer. The main objectives of this thesis are to determine heat transfer coefficient for nanofluid with inserted tape through experiment. Also, this paper will compare the experimental value of heat transfer coefficient with pervious literature. The thesis described the methodology utilize and the expected result from the experiment. Reynolds number varies between 4 000 until 22 000 within turbulent region, on the other hands, nanoparticles used is Alumina, Al_2O_3 with volume concentration of 0.5%. The dimension of the twisted tape inserts used is 5, 10, 15 and 83. From the experimental result, ratio of twist, H/D =10 for nanofluid provides higher Nusselt number for higher Reynolds number. Theoretically, H/D of 5 for nanofluid should have highest value of Nusselt number. Different result than theory is due to environment distraction. Using twist insert tape with nanofluid as working fluid, the value of Nusselt number is higher compare to previous literature of Nusselt number for nanofluid and water in plain tube by 33.51% and 42.17% respectively. The research paper concluded with tabulation from result and recommendation for further research.

ABSTRAK

Tesis ini berkaitan dengan kajian pekali perpindahan panas nanofluid dengan pita dimasukkan. Penyelidikan dan pembangunan untuk pemindahan peningkatan panas menggunakan nanofluid menunjukkan reaksi positif untuk meningkatkan laju perpindahan panas konveksi. Tujuan utama dari tesis ini adalah untuk menentukan pekali perpindahan panas, untuk nanofluid dengan pita dimasukkan melalui eksperimen. Selain itu, makalah ini akan membandingkan nilai percubaan pekali perpindahan panas dengan literatur yg dpt tembus. Tesis ini menggambarkan metodologi memanfaatkan dan hasil yang diharapkan daripada percubaan. bilangan Reynolds berbeza-beza antara 4 sampai dengan 22 000 000 di kawasan bergolak, di tangan lain, nanopartikel yang digunakan adalah Alumina, Al2O3 dengan konsentrasi 0,5% kelantangan. Dimensi dari pita sisipan twisted yang digunakan adalah 5, 10, 15 dan 83. Dari hasil percubaan, nisbah twist, H / D = 10 untuk nanofluid menyediakan jumlah yang lebih tinggi Nusselt untuk nombor Reynolds yang lebih tinggi. Secara teoritis, H / D 5 untuk nanofluid harus mempunyai nilai tertinggi bilangan Nusselt. Keputusan Berbeza dengan teori adalah kerana gangguan persekitaran. Menggunakan tape memasukkan twist dengan nanofluid sebagai bendalir kerja, nilai bilangan Nusselt lebih tinggi berbanding dengan kesusasteraan dahulu bilangan Nusselt untuk nanofluid dan air dalam tabung biasa sebanyak 33,51% dan 42,17% masing-masing. Kertas kajian menyimpulkan dengan tabulasi dari hasil dan cadangan untuk kajian lebih lanjut.

TABLE OF CONTENTS

CHAPTER 4 RESULT

CHAPTER 5 CONCLUSION AND RECOMMENDATIONS

LIST OF TABLES

LIST OF FIGURES

LIST OF SYMBOLS

$\dot{Q}$	Rate of heat transfer, (kJ/s)
$\dot{Q}_{conv}$	Heat convection rate, (kJ/s)
h	Convection heat transfer coefficient, ($W/m^2 . {}^{\circ}C$)
A_s	Heat transfer surface area, (m^2)
T_s	Surface temperature, ($^{\circ}C$)
T_∞	Temperature of the fluid, ($^{\circ}C$)
L_h	Hydrodynamic entry length, (m)
μ	Dynamic viscosity of the fluid, ($Pa{\cdot}s$ or $N{\cdot}s/m^2$)
$\dot{m}$	Mass flow rate, (kg/s)
V_{ang}	Average fluid velocity, (m/s)
L_t	Thermal entry length, (m)
r	Radius of circular tube, (m)
T_m	Mean temperature, ($^{\circ}C$)
T_i	Inlet temperature, ($^{\circ}C$)
T_e	Outlet temperature, ($^{\circ}C$)
A_c	Plate cross-section area, (m^2)
$\dot{m}$	Mass flow rate, (kg/s)
ρ	Density of the fluid, (kg/m^3)
$\dot{V}$	Volumetric flow rate, (m^3/s)
ΔT_{avg}	Average of the temperature differences between the surface and the fluid at the inlet and the exit of the tube, ($^{\circ}C$)
ΔT_m	Mean temperature difference, ($^{\circ}C$)
$\dot{q}$	Heat flux, (W/m^2)

C_p	Constant pressure specific heat, ($kJ/kg.K$)
ΔP	Pressure drop
ΔP_L	Pressure losses due to viscous effect
f	Darcy friction factor
D	Tube diameter, (m)
Re	Reynolds number
Pr	Prandtl number
ΔT	Temperature different, (K)
T_w	Wall temperature, ($^{\circ}C$)
υ	Kinematic viscosity, ($\upsilon = \mu / \rho$), (m^2/s)
k	Thermal conductivity, ($W/m.K$)
Nu	Nusselt number
ϕ	Volume Concentration, (%)
D_i	Inlet Diameter, (m)
T_b	Bulk temperature, ($^{\circ}C$)

LIST OF ABBREVIATIONS

FKM	Fakulti Kejuruteraan Mekanikal
FYP	Final year project
HTC	Heat Transfer Coefficient
USA	United States of America
Eq	Equation

CHAPTER 1

INTRODUCTION

1.1 RESEARCH BACKGROUND

Advancement of thermal field and nanotechnology urged researchers to do more research on Nanofluid following major trend in modern science and technology which is miniaturization industries. During earlier research, there had been research to have millimetre and micrometer size of particle in order to enhance the rate of heat transferring but there have been problem by means clogging and suspension stability. The invention does not stop there. Recently, all industrial sectors significant the roles of forced convective heat transfer. There are many different techniques to determine the abilities of heat transfer for nanofluid suggested by other researcher such as through experimental data, theoretical formula and others. Furthermore, with the availability of nanofluid as fluid which much more reliable to be used, further research within this field have been done.

Forced convective heat transfer of nanofluid is the heat transfer between a forced flowing nanofluid through a confined region and confining wall. Some examples of convective heat transfer application is cooling of microelectronics, process intensification in the chemical industry, heat exchange with waste heat recovery in power plants and cooling of car engines.

Nanofluid can be understood as nanoparticles in based fluid which have ability to transfer heat efficiently than other traditional heat fluid such as water. The capability of heat transfer is based on its property, dimensions and also volume fraction (Sundar et al., 2007). Using different concentration of nanofluid with interested flow region such

as laminar, transition and turbulent, it yield different research paper. Through observation on flow of nanofluids in a tube, enhancement of heat transfer has been found and supported by previous researcher. Smithberg and Landis (1964), Lopina and Bergles (1969) , Manglik and Berles (1993), Sarma et al. (2002), Sarma et al. (2003) have reported heat transfer enhancements with twisted tape inserts of single phase fluids in a tube. Sundar and Sharma (2010) concluded that heat transfer coefficient and friction factor of 0.5% volume concentration of Al_2O_3 nanofluid with twist ratio of five is 33.51% and 1.096 times respectively higher compared to flow of water in a tube. Hence, the present study is undertaken to obtain experimental data with help of twisted tape in plain tube using nanofluids and compare with previous literature.

1.2 PROBLEM STATEMENT

Currently, majority of the industries using the cooling system with traditional heat transfer fluid such as water in the heat exchanger. Thus, the rate of heat transfer can be increased by using nanofluid as the heat transfer fluid and minimize the heat exchanger pumping power. This reduces losses in profits and following the principles of ergonomics. Conventionally, the industrial will add inserted tape in the tube with traditional heat transfer fluid such as oil, water and ethylene glycol to enhance the heat transfer. Even though, the flow will be facing disturbance and friction, the friction can be reduce by using smaller particles which nowadays, the smallest particles that industrial can use is nanoparticles. Moreover, by using inserted tape, it acts as passive inducer of convection heat transfer. Further research has to be done in this field to maximize the nanofluid convection heat transfer ability.

1.3 SIGNIFICANCE OF STUDY

After achieving the objectives, the manufacturing industry will have an alternative method in saving the cost of production and increasing the rate of production. By determining the heat transfer coefficient, the industrial could use the method to control the rate of heat transfer for cooling system such as heat transfer in heat exchanger. In normal situation, workers that handle the heat exchanger must have specific experience and skills. This study also helps the non-experience worker to

handle the heat exchanger in obtaining the optimum rate of heat transfer. On the other hands, using nanofluid as the heat transfer fluid minimize the friction in the tube. Thus, a further study is needed in order to accomplish the vision and within given the limitation. Some of the research question that has been proposed through this paper is method to determine the coefficient of heat transfer for nanofluid with inserted tape. The paper also will discuss on the effect of inserted tape with 180˚ of turning.

1.4 RESEARCH OBJECTIVE

The objectives of this paper are as follows:

i. Determination of heat transfer coefficient for nanofluid with inserted tape through experiment.
ii. Observe and compare the experimental value of heat transfer coefficient from previous literature.

1.5 RESEARCH SCOPES

For the main purpose of this research, the following scopes are developed:

i. To create turbulent flow, high Reynolds number used in range 4000 to 22 000.
ii. Nanoparticles used is Alumina, Al_2O_3.
iii. The volume concentration of nanofluid examine is 0.5%.
iv. The flow of nanofluid used in this paper is under fully developed region.
v. The behaviour of flow disturb by twisted tape with 180˚ of turning.
vi. Twisted tape have ratio within 5, 15, 20, and 83.

1.6 PROCESS FLOW CHART

Figure 1.1 shows the connection between the different stages of the process or parts of the system along the study. This provides clear image of the research being done for FYP 1 and FYP 2.

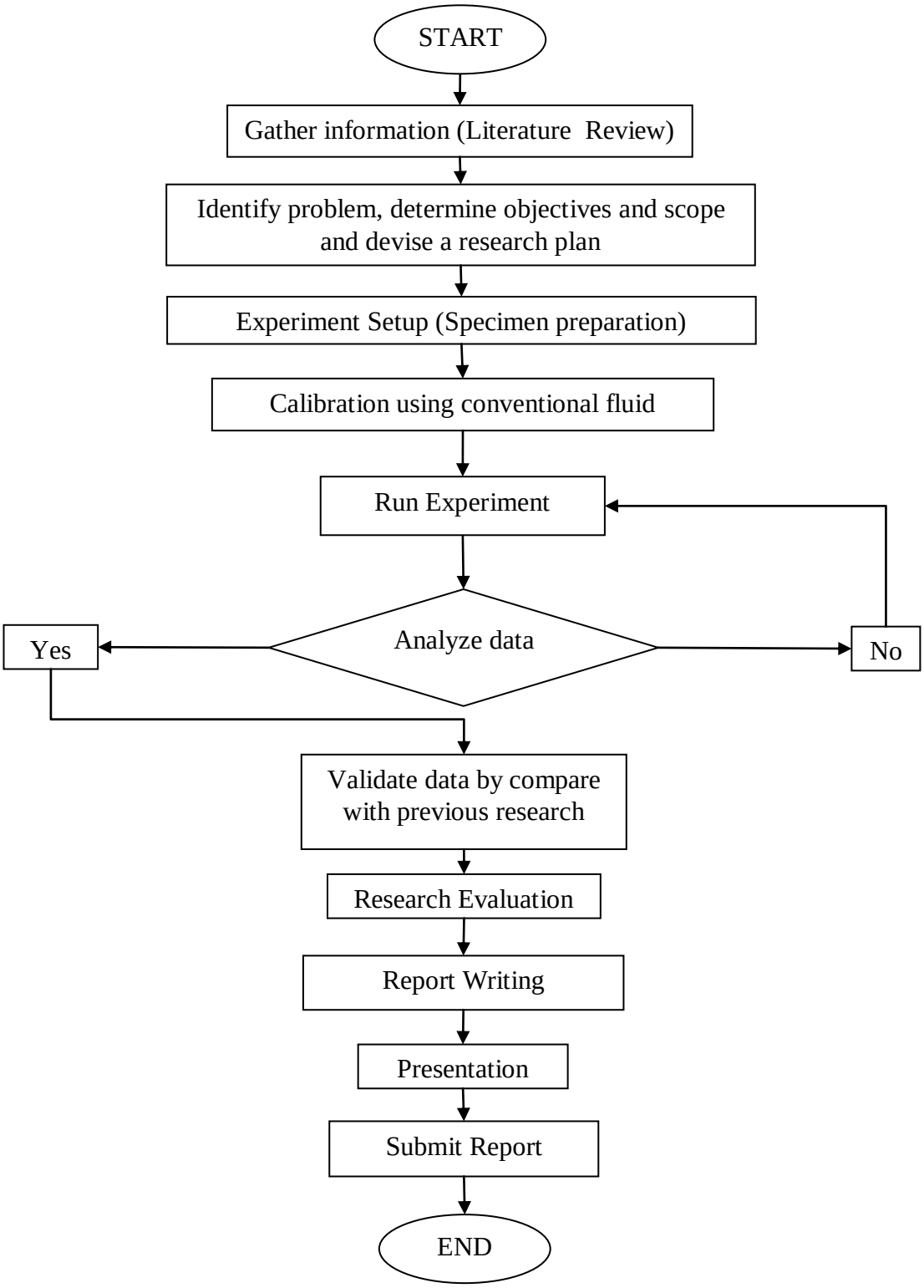

Figure 1.1: Flow diagram of the research

CHAPTER 2

LITERATURE REVIEW

2.1 INTRODUCTION

A converging focused literature review within a related field or interest of research is one of the most essential activities in the procedure of completing a research. In order to produce a productive literature review, it is recommended to include the historical perspective, selected heat transfer mechanism with understanding classification of fluid flow which the research paper concerns more on internal forced convection for inserted tape in a tube with turbulent flow. Also, review on previous studies related within the scope as additional guidance for the research paper also its application from engineering perspective. Besides that, discussion of some information on the technology and equipment that used for this study case such as Nanofluid and Twisted Tape are included. By considering the related engineering parameters used in through this research paper, relationships between the parameter are also discussed. Not only elaborate on the parameters, it covers the relationship on the parameters before meets the conclusion for this chapter. Hence, this chapter acts as a platform of reviews to support and define each action performed during the experiment being held.

2.2 HEAT TRANSFER

Heat transfer can be seen throughout our daily life. Human body as the easiest example, constantly rejecting heat to its surrounding ensuring that it is comfortable with the surrounding. Heat transfer can be classified as the science that deals with the determination of the rates of energy transfer. The interested energy is heat which can be defines as the form of energy that can be transferred from one system to another as a

result of temperature difference (Cengel, 2006). For heat transfer to occur, temperature difference is the basic requirement. With the knowledge of heat transfer, the rates of heat transfer to or from a system can be determine thus the times need of heating or cooling as well as the variation of temperature can be known either through experimental method or theoretical method with some assumption need to be done first.

2.3 HEAT TRANSFER MECHANISM

As been discussed in previous section, heat can be define as the form of energy that can be transfer from one body to another caused by temperature defences as the forcing force. Thermodynamics field known to be concern with the amount of energy transfer as a system changes from equilibrium state to another (Incropera et al., 2007). We also understand that heat transfer is the science field which concerns more with the determination of the rates of heat transfer. Hence, the industrial can invents the optimal insulation thickness or determined the basis of heat transfer analysis considering the economical aspects.

The heat transfer can be occurred in three different modes which are conduction, convection and radiation. All of it needs temperature difference with heat transfer from high-temperature body to the lower-temperature one. The clear differences among them are conduction is due to collisions, diffusions or vibrations of the random motion molecules contrast with convection which occur as effect of conduction and fluid motion. Figure 2.1 shows heat transfer by convection and conduction. On the other hands, radiation does not need any medium to be occurred since the radiation, itself can be occurred in a vacuum condition. Throughout the research paper, the interested mechanism is convection only.

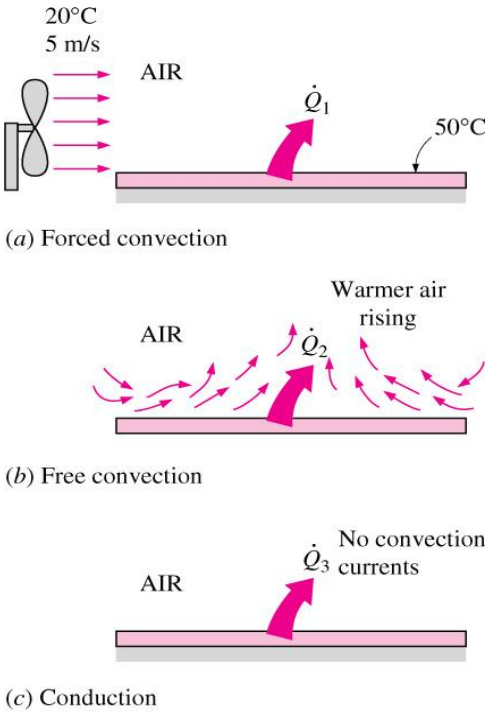

Figure 2.1: Heat transfer from a hot surface to the surrounding fluid by convection and conduction.

Source: Cengel, (2006).

Within our surrounding, there are a lot of convection process happen without we realise such as process of drying the clothes, cooling a hot water or hot surface with our without external force and others. These are some example of application of heat convection in our daily life. Convection also gives benefits to the industrial field. With convection process, the cooling system has been built either used to cool the engine of a car of cooling a heat exchanger unit. Therefore, convection gives chances for human to utilize the cooling system in order to produce a machine that can run smoothly without corrupt because of heat.

Heat convection can be define as the mode of energy transfer between solid surface and the adjacent liquid or gas that is in motion, and it involves the combined effects of conduction and fluid motion. (Cengel, 2006) Since our surrounding does include solid and fluid that have motion, convection process is easily happen whereas, to convection happens, there must be a surface which is solid in contact with liquid or

gas in motion. To have a greater effect of convection, the fluid motion must be faster. The heat transfer between solid surface and the fluid are enhance by the presence of bulk motion of the fluid. Also, the determination of heat transfer rates can be done.

2.4 THEORY OF CONVECTION HEAT TRASFER

In order to study the heat transfer coefficient, first and foremost, deep understanding in theoretical is a must. There are several theory related with convection heat transfer which are concern within this report such as Newton's cooling law, internal force flow, boundary layer, mean velocity, surface temperature, heat flux and pressure drop. All elaborated theories are related to one another. By converging towards the objectives of this research, each theory is being discussed to get a clearer view.

2.4.1 Newton's Law of Cooling

Newton's Law of Cooling states that the rate of change of the temperature of an object is proportional to the difference between its own temperature and the ambient temperature (Incropera, 2007). By means, Newton's Law makes a statement about an instantaneous rate of change of the temperature. Formula below states the law:

$$\dot{Q}_{Conv} = hA_s\left(T_s - T_\infty\right) \tag{2.1}$$

Where h is the local convection heat transfer coefficient, heat transfer surface area, A_s, temperature of the surface, T_s, and temperature of the fluid sufficiently far from the surface or ambient temperature, T_∞.

2.4.2 Internal Forced Convection

In Internal forced convection, the fluid has a moving motion in flow sections of circular cross section or noncircular cross section which are referred as pipes and ducts, caused perhaps by a pump or fan or other driving force independent of the body. Figure 2.2 shows an example of a pipe and a duct. Circular pipes can withstand large pressure

differences between the inside and outside without undergoing any significant distortion, but non circular pipes cannot.

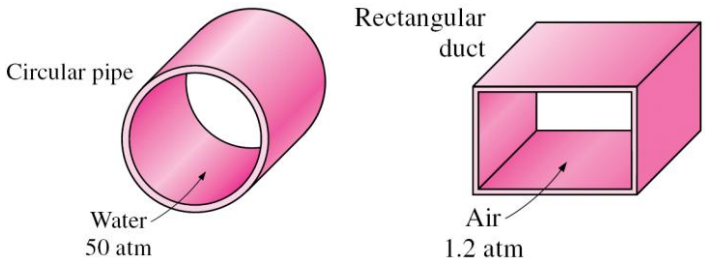

Figure 2.2: Example of circular pipe and rectangular duct.

Source: Cengel, (2006).

2.4.3 The Entry Region

If a fluid enters a circular pipe at a uniform velocity, due to no-slip condition, the fluid particles in the layer creates contact with the surface of the pipe come to a complete stop. As a result, a velocity gradient develops along the pipe. The velocity boundary layer is the region of flow which the effects of the viscous shearing forces caused by fluid viscosity are felt. The region from the pipe inlet to the point at which the boundary layer merges at the centreline is called as hydrodynamic entrance region, and the length of this region is called as the hydrodynamic entry length, L_h. The profile of velocity in the fully developed region for laminar region is parabolic and for turbulent flow is flatter or fuller due to eddy motion and more vigorous mixing in radial direction. Figure 2.3 shows velocity boundary layer in a tube.

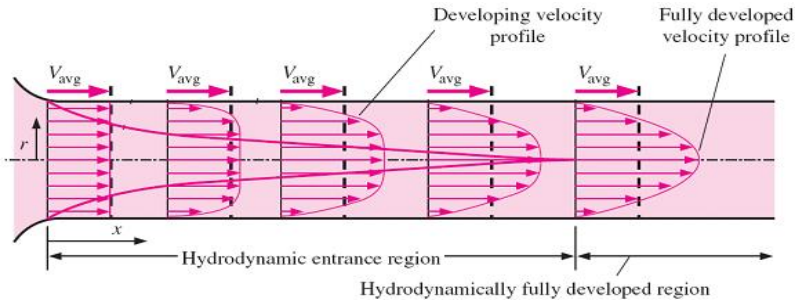

Figure 2.3: Boundary Layer for Entrance Region

Source: Cengel, (2006).

The region of flow over which the thermal boundary layer develops and reaches the tube centre is called as thermal entrance region and the length of this region is called as thermal entry length, L_t. The region beyond the thermal entrance region in which the dimensionless temperature profile expressed as $(T_s - T)/ (T_s - T_m)$ remains unchanged is called as the thermal the thermally fully developed region. For fully developed flow, it contains both hydrodynamically and thermally developed and thus both the velocity and dimensionless temperature profile remain unchanged. Figure 2.4 shows thermal boundary layer in a tube.

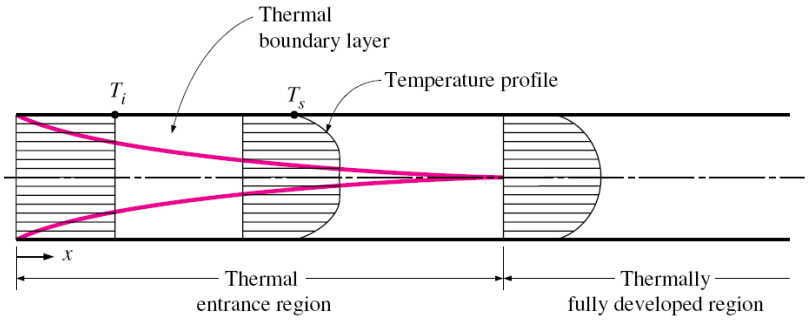

Figure 2.4: Developing Thermal Boundary Layer in Tube.

Source: Cengel, (2006).

2.4.4 Mean Velocity

Owing to varies of velocity over the cross section and there is no well-defined free stream, it is necessary to work with a mean velocity, V_{avg} when dealing with internal flows. This velocity is defined such that, when multiplied by the fluid density, ρ and the cross-sectional area of the tube, A_c it provides the rate of mass flow, $\dot{m}$ through the tube. Hence, Eq. 2.2 shows the equation of rate of mass flow from Cengel (2006) where average flow rate can be applied.

$$\dot{m} = \rho \dot{V} = \rho A_c V_{avg} \tag{2.2}$$

The fluid velocity in a tube changes from zero at the surface because of the no-slip condition to a maximum at the centre of tube. It is more convenient to work with mean velocity or an average velocity, V_{avg} for fluid flow which remains constant in incompressible flow when constant cross-sectional tube. Through Figure 2.5, diagram of average velocity for fully develop flow could be understand.

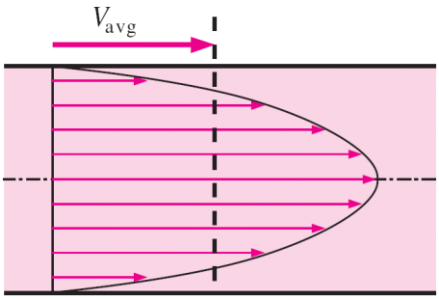

Figure 2.5: Average Velocity for Fully Develop Flow

Source: Cengel, (2006).

2.4.5 Surface Temperature

For constant surface temperature, the Newton's law of cooling, to or from a fluid flowing in a tube can be expressed as

$$\dot{Q} = hA_s \Delta T_{avg} = hA_s \left(T_s - T_m\right)_{avg} \tag{2.3}$$

Where the arithmetic mean temperature difference, ΔT_m can used to express ΔT_{avg} as follows;

$$\Delta T_{avg} \approx \Delta T_m = \frac{\left(T_s - T_i\right) + \left(T_s - T_e\right)}{2} \tag{2.4}$$

By understanding the expression of arithmetic mean temperature difference, ΔT_{lm} is the average of the temperature differences between the surface and the fluid at the inlet and the exit of the tube. The result can be accepted, but not always. Thus, a better way of evaluating ΔT_{avg}, using the logarithmic mean temperature difference, ΔT_{lm} the rate of heat transfer can be present as below,

$$\dot{Q} = mC_p = hA_s \Delta T_{lm} \tag{2.5}$$

Where, ΔT_{lm} is express in equation below.

$$\Delta T_{lm} = \frac{T_i - T_e}{ln\left[\left(T_s - T_e\right)/\left(T_s - T_i\right)\right]} = \frac{\Delta T_e - \Delta T_i}{ln\left[\Delta T_e / \Delta T_i\right]} \tag{2.6}$$

2.4.6 Heat Flux

For constant heat flux, it's simplify on determine total heat transfer rate,

$$\dot{Q} = \dot{q}_s A_s = \dot{m} C_p \left(T_e - T_i\right) \tag{2.7}$$

Note that, T_e is the temperature exit and T_i is the temperature inlet. Thus, the mean fluid temperature at the tube exit can be written as,

$$T_e = T_i + \frac{\dot{q}_s A_s}{\dot{m} C_p} \tag{2.8}$$

Where the surface temperature for constant heat flux can be determine from below equation

$$\dot{q}_s = h(T_s - T_m) \rightarrow T_s = T_m + \frac{\dot{q}_s}{h} \tag{2.9}$$

Figure 2.6 shows surface temperature T_s will also increase linearly in the flow direction since both $\dot{q}_s$and h are constant and thus $T_s - T_m$ will be constant.

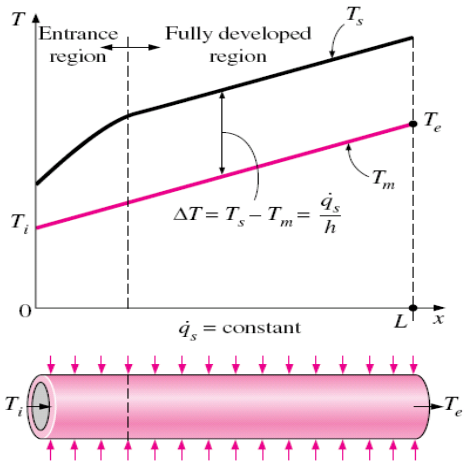

Figure 2.6: Variation of the tube surface and the mean fluid temperature under constant heat flux conditions

Source: Cengel, (2006)

2.4.7 Pressure Drop

The power requirements of the fan or pump to maintain flow can be determine based on pressure drop, ΔP and its can denoted as the difference between final and initial of pressure. To emphasize that it is a loss due to viscous effect, pressure drop is called pressure losses indicated by ΔP_L.

For fully develop internal flows (laminar and turbulent flows, circular or noncircular pipes, smooth or rough surfaces, horizontal or inclined pipes), the pressure drop can be expressed as shown below

$$\Delta P_L = f \frac{L}{D} \frac{V_{avg}^2}{2} \tag{2.10}$$

With, *f* is the Darcy friction factor or Darcy-Weisbach friction factor. But, solving for *f* gives the friction factor only valid for fully developed laminar flow in a circular tube. The equation as follows:

$$f = \frac{64\mu}{\rho D V_{avg}} = \frac{64}{Re} \tag{2.11}$$

To determine the friction factor for turbulent flow, the Colebrook equation is used so that the pressure drop can be calculated.

$$\frac{1}{\sqrt{f}} = -2.0 \log\left(\frac{\varepsilon / D}{3.7} + \frac{2.51}{Re\sqrt{f}} \right) \tag{2.12}$$

Where, ε is relative roughness of the material and different value with different material. It is present Darcy friction factor for pipe flow as a function of the Reynolds number and ε/D over a wide range also one of the accepted and used charts in engineering.

Once the pressure loss is known, the required pumping power to overcome the pressure loss can be determine

2.5 CLASSIFICATION OF FLUID FLOW

Fluid flow can be very smooth, calm, and regular, but generally the flow of a fluid is not so disciplined, it becomes a vagabond and starts flowing in random patterns. While studying the motion of a rigid body we do not have to bother about the relative motion of the particles of the rigid body as they are very firmly fixed to each other and

move as a whole. But for the study of the motion of fluids, things are not so simple because the fluid particles are attached with each other with very weak forces. There are various relative motions and a lot of possibilities for relative motion between the fluid particles. Since convection heat transfer have closed bond with fluid mechanics, the science that deals with the behaviour of fluids at rest or in motion, there is a wide variety of fluid problems encountered in our daily practice. As a convenient way, they are classified to certain basis of common characteristics to make it easy to be study.

Some smooth layers of fluid and orderly flows are known as laminar while others flow which is highly disordered flows occurs at high velocities is called turbulent. A flow that contains overlapping laminar and turbulent flows is known as transitional. The required power for pumping the flow does influence by the flow regime. The characteristics that are concern most in this research is internal forced flow with turbulence characteristics.

2.5.1 Laminar Flow

When highly viscous fluids such as oils flow in small diameter tubes or narrow passages, laminar flow is encountered. Although, laminar region is not the case in practice since most pipe flows encountered in practice are turbulent. Under most practical conditions, the flow in a tube is laminar for Re < 2300 where Reynolds number could relate between the average velocity of the flow and the flow's properties. Deeper discussion regarding Reynolds number could be found in section 2.8.2 from the same chapter.

Edwards et al., (1979) determined the average Nusselt number in thermal entrance region for a circular tube of length, *L* subjected to constant surface temperature is stated as follows;

$$Nu = 3.66 + \frac{0.065(D/L)RePr}{1+0.04[(D/L)RePr]^{2/3}} \tag{2.13}$$

The relation assumes that the flow is hydrodynamically developed when the fluid enters the heating section, but it can also be used approximately for flow developing hydrodynamically.

2.5.3 Turbulent Flow

As the flow speed of the otherwise calm layers increases, these smoothly moving layers start moving randomly, and with further increase in flow velocity, the flow of fluid particles becomes completely random and no such laminar layers exist anymore. Shear stresses in the Turbulent Flow are more than those in Laminar Flow. A dimensionless parameter, Reynolds Number, is defined as the ratio of inertial and viscous force to characterize these two types of flow patterns. With increase in flow velocity the initial forces increase so the Reynolds Number.

Since the analysis of turbulent flow conditions is a good deal more involved, greater emphasis is placed on determining empirical correlations. For fully developed turbulent flow in smooth tubes, Dittus-Boelter equation (Dittus and Boelter, 1930) shown in below;

$$Nu = 0.023 Re^{0.8} Pr^{n} = \begin{Bmatrix} Re > 10,000,\ n = 0.4\, heating \\ 0.7 \le Pr \le 160,\ n = 0.3\, cooling \end{Bmatrix} \tag{2.14}$$

Another equation that improved from Dittus-Boelter equation is Gnielinski equation (Gnielinski, 1976) as follows;

$$Nu = \frac{\left(\frac{f}{2}\right)(Re - 1000)\, Pr}{1 + 12.7\left(\frac{f}{2}\right)^{0.5}\left(Pr^{\frac{2}{3}} - 1\right)} \tag{2.15}$$

Where the friction factor, f can be determine using Fanning friction factor.

$$f = (1.58 \ln Re - 3.82)^{-2} \tag{2.16}$$

2.6 INTRODUCTION TO NANOFLUIDS

After a century, it has been one of the great challenges on heat transfer field struggling on how to enhance industrial heat transfer by fluid mechanics, the low thermal conductivity of conventional fluids as water, oil, and Ethylene-Glycol (EG) for transferring the heat. Seeing a hope through Maxwell's research during 1873, which shows the possibilities of increasing thermal conductivity of a fluid-solid mixture by increasing volume fraction of solid particles, further research using particles with micrometer or even millimetre dimensions were used (Izadi, 2009). Though, several problems such as abrasion, clogging and pressure losses were caused by those particles. Through the past decade, technology to prepare particles in nano-meter dimensions was improved. The nanoparticles are significant with size smaller than 100nm and differ from conventional particles (millimetre or micro-scale).

An interesting filed of heat transfer problems that require nanoscale consideration in analysis, is that of thermal phenomena in nanomaterials including nanofluids or nanoparticles suspensions obtained by introducing nanometer-sized solid particles in solid matrices or liquids (Sobhan, 2008).

A group in Argonne National Laboratory USA (Choi, 1995) was the first research group describe liquid suspensions containing nanoparticles with thermal conductivities higher than base liquids as nanofluids. Nanofluid can be used to enhance heat transfer in separated regions which can be accomplished by increasing the value of convective heat transfer coefficient or Nusselt number in separated flow.

Today, a variety of nanometer-sized particles have been made from common metal or metal oxide materials, as well as from compounds such as ZnO, ZnS, CdSe, Cd_3P_2, Zn_3P_2, PbI_2, HgI_2, BiL_3, and GaN. The diameters of the particles range from several nanometers to several hundred nanometers and can be produced in a highly reliable process that can accurately control the composition, shape, and size of the particles. Figure 2.7 showing SEM image of nanoparticles used in this research paper, Al_2O_3.

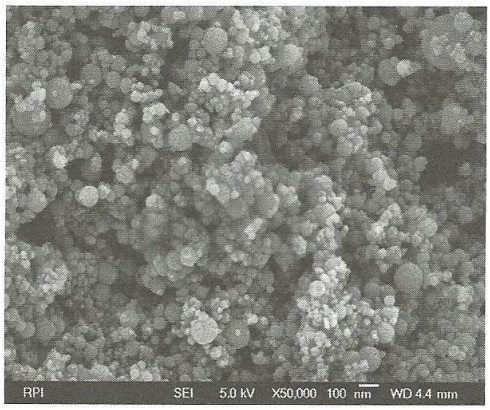

Figure 2.7: SEM image of Al_2O_3 nanoparticles

Source: Sobhan, (2008)

2.6.1 Nanofluid Application

The miniaturization of mechanical and electrical components creates a need for improved heat transfer characteristics in current cooling fluids. These involve area where heat transfer analysis can be used to develop optimal control strategies for end-user applications, and where heat transfer analysis can be used to effectively produce and optimize manufacturing process for systems and structures. Nanofluid have the potential to be used as cooling fluids since the nanoparticles suspensions are not abrasive and will not clog mechanical components. These fluids have also shown to exhibit substantially higher thermal conductivities compared to the conventional heat transfer fluids. Some useful applications for nanofluid are as alternative coolants, greases, or lubricants in automotive applications, coolants for microelectronics and others. Besides that few example where nanoscale heat transfer can also be used in diverse areas such as biotechnology, nanotechnology (nanofabrication, nanomaterials synthesis), energy conversion and power generation systems such as heat exchanger systems, photovoltaic conversion and thermoelectric energy conversion system, optoelectronics and, in general, every application that involves miniaturization as an objective.

2.6.2 Advantage and Disadvantage of Nanofluid

Nanofluid is can be considered as one of excellent heat transfer working fluid due to its capability of heat transfer. Still, there are advantages and disadvantages of using nanofluid. The good thing of using nanofluid is, nanofluid have great capability to act as heat transfer enhancement since the particles that used in nano size which very small. Thus, the shear stress between the particles and the wall can be neglected. Thus, its works nearly as perfect heat transfer enhancer. However, nanofluid is hard to be manufacture. Only minority of the industries become its manufacturer, thus, the price is overwhelming. To use it in industrial as application, some of the financial manager would say that it is impractical and not economical. Besides that, nanofluid production faces some major challenges such as agglomeration of particles in solution and the rapid settling of particles in fluids.

2.7 PREPARATION OF NANOFLUIDS

Mixing nanoparticles with a fluid where the nanoparticles remain in suspension for a long time are termed as ‘nanofluids’ and understand as nanoparticles in suspensions. Several studies, including the earliest investigations of nanofluids, used a two-step method in which nanoparticles or nanotubes are first produced as a dry powder and then dispersed into a fluid in a second processing step. In contrast, the one-step method entails the synthesis of nanoparticles directly in the heat transfer fluid.

2.7.1 Two-step method

The preparation of nanofluids begins by direct mixing of the base fluid with the nanomaterials. In the first step, nanomaterials are synthesized and obtained as powders, which are then introduced to the base fluid in a second step. This is because the concentration and size distribution can be controlled. Changing the pH value of the suspension, adding surfactants or a suitable surface activator, or using ultrasonic or microwave vibration, are all techniques that have been used with two-step method to have better disperse and more evenly distribute the nanoparticles in the base fluid and maintain the stability of the suspension (Sobhan, 2008). Theoretically, as nanoparticles

used are small, the weight to volume ratio is suitable, and the dispersion method s applied correctly, the nanoparticles will be very well dispersed and suspension will be stable for several days. However, majority research paper reported that the suspension sample can be maintained in a homogenous stable state for no more 24 hours.

2.7.2 One-step method

The one step method is the method where nanoparticles are produced directly in the base fluid to obtain suspension. The drawbacks of this technique however, are that the use of low vapor pressure liquids are essential and only limited quantities can be produced.

2.8 ENGINEERING PARAMETERS

There are certain parameters of engineering that are going to be used along this research paper. Majority of them are from knowledge of thermodynamics and heat transfer. Each of them related with each other in order to validate the result.

2.8.1 Heat Transfer Coefficient

The convection heat transfer coefficient, h is dependent on the type of media, gas or liquid, the flow properties such as velocity, viscosity and other flow and temperature dependent properties. The important parameters in forced convection heat transfer analysis are from Newton's Law of Cooling as shown in Eq. 2.1 which could be rearranged as:

$$h = \frac{\dot{Q}}{A_s \left(T_w - T_\infty \right)} \tag{2.17}$$

Where surface temperature, T_s, is taken at wall temperature, T_w with the rate of heat transferred to the surrounding fluid is proportional to the exposed area of the object and the difference between the object temperature and fluid free-stream temperature.

The constant of proportionality, *h* is termed as the convection heat transfer coefficient. Other terms describing *h* include film coefficient and film conductance.

2.8.2 Reynolds number

Depending on the flow condition, the flow in a tube can be laminar or turbulent. Thus in this research paper, turbulent flow need to be obtain in order to full-fill its requirement. With circular tube, Reynolds numbers is defined as

$$Re = \frac{\rho V_{avg} D}{\mu} \tag{2.18}$$

For flow through circular tubes, the hydraulic diameter influence the friction factor which is define as,

$$D_h = \frac{4A_c}{p} \tag{2.19}$$

$$D_h = \frac{4(\pi D^2 / 4)}{\pi D} = D \tag{2.20}$$

It certainly desirable to have precise number of Reynolds for laminar, transitional and turbulent flows, but this is impractical since they also depend on surface roughness, pipe vibrations and the fluctuations in the flow. Practically, Re > 10,000 for fully turbulent flow.

2.8.3 Prandtl number

The Prandtl Number is a dimensionless number approximating the ratio of momentum diffusivity (kinematic viscosity) and thermal diffusivity and can be expressed as:

$$Pr = \frac{\upsilon}{\alpha} = \frac{\mu C_p}{k} \tag{2.21}$$

Range of Prandtl number is from less than 0.01 for liquid metals to more than 100 000 for heavy oils (Cengel, 2006). The Prandtl Number is often used in heat transfer and free & forced convection calculations.

2.8.4 Nusselt Number

The traditional dimensionless from of *h* is the Nusselt number *Nu*, which may be defined as the ratio of convection heat transfer to fluid conduction heat transfer under the same conditions. We define the Nusselt number as the ratio of these two:

$$Nu = \frac{\dot{q}\left(convection\right)}{\dot{q}\left(conduction\right)} = \frac{hD_i}{k} \tag{2.22}$$

A Nusselt number of order unity would indicate a sluggish motion little more effective than pure fluid conduction: for example, laminar flow in a long pipe. A large Nusselt number means very efficient convection: For example, turbulent pipe flow yields *Nu* of order 100 to 1000. Hence, Nusselt number for turbulent flow has been discussed in previous subchapter, 2.5.3.

Sarma et al. (2009) has developed regression Nusselt number valid for both water and nanofluid having volume concentration less than 0.1%. Since the research interested in volume concentration 0.5% which is less than 0.1%, hence, the equation give as follows:

$$Nu_{reg} = 3.138\times10^{-3}(Re)(Pr)^{0.6}(1.0+H/D)^{0.03}(1+\phi)^{1.22} \tag{2.23}$$

Where *H/D* is twisted tape ratio and ϕ is volume concentration in %. Both characteristics are discussed further in next chapter.

2.8.5 Relationship between the Parameters

From the parameters used in this paper, the heat transfer coefficient can be determine with Reynolds numbers be higher than 10 000 in order to create turbulent

flow for internal flow in the tube and forced by generated pump. Nusselt number can show the relationship of Reynolds number and Prandtl number.

2.9 THEMOPHYSICAL PROPERTIES

Thermophysical properties do influence the analysis of heat transfer coefficient incoincidently. The properties used in this paper are dynamic viscosity, thermal conductivity, density and specific heat. To check the apparatus availability, regression equation for water developed by Azmi et al., (2010) are used as the thermophysical properties of water. The regression equations for water are shown as Eq. 2.24 until 2.27.

For Dynamic Viscosity, (Azmi et al., 2010)

$$\mu_w = 0.00169 - 4.25263\times10^{-5}T_b + 4.9255\times10^{-7}\left(T_b\right)^2 - 2.0993504\times10^{-9}\left(T_b\right)^3 \quad (2.24)$$

For Thermal Conductivity, (Azmi et al., 2010)

$$k_w = 0.56112 + 0.00193T_b - 2.60152749\times10^{-6}\left(T_b\right)^2 - 6.08803\times10^{-8}\left(T_b\right)^3 \quad (2.25)$$

For Density, (Azmi et al., 2010)

$$\rho_w = 1000\left[1.0 - \frac{\left(T_b - 4.0\right)^2}{119000 + 1365T_b - 4\times\left(T_b\right)^2}\right] \quad (2.26)$$

For Specific Heat, (Azmi et al., 2010)

$$C_w = 4217.629 - 3.20888T_b + 0.09503\left(T_b\right)^2 - 0.00132\left(T_b\right)^3 + 9.415\times10^{-6}\left(T_b\right)^4 - 2.5479\times10^{-8}\left(T_b\right)^5 \quad (2.27)$$

Some papers have published regression equation for nanofluid. Below are the equations used for the analysis as Eq. 2.28 until 2.31:

For Dynamic Viscosity, (Azmi et al., 2010)

$$\frac{\mu_{nf}}{\mu_w} = 0.9042 + 0.1245\ \phi + 0.6436 \times \left(\frac{d_p}{d_{max}}\right) - 0.08445 \times \left(\frac{T_b}{T_{max}}\right) \quad (2.28)$$

For Thermal Conductivity, (Azmi et al., 2010)

$$\frac{k_{nf}}{k_w} = 0.9808 + 0.0142\phi + 0.2718 \times \left(\frac{T_b}{T_{max}}\right) - 0.1020 \times \left(\frac{d_p}{d_{max}}\right) \quad (2.29)$$

For Density, (Taufiq, 2010)

$$\frac{\rho_{nf}}{\rho_w} = 0.9988 + 0.03485\phi + 0.002217\left(\frac{T_b}{70}\right) \quad (2.30)$$

For Specific Heat, (Taufiq, 2010)

$$\frac{C_{pnf}}{C_{pw}} = 0.9977 - 0.03344\phi - 0.001111\left(\frac{T_b}{70}\right) \quad (2.31)$$

2.10 PREVIOUS STUDIES

A number of experimental studies have been performed to investigate the transport properties of nanofluids. Numerical regression equation and simulation paper were result of further research from the experimental studies. Through this research paper, previous studies related are being discussed here.

Sundar et al., (2007) did some research related with nanofluid which is investigation of heat transfer enhancements with Al_2O_3 nanofluids for twisted tape insert in a circular tube. The journal paper is the main reference to be used since the experimental procedure is similar with the research paper suggested. By using γ- Al_2O_3 which had been kept in deionized water were investigated at different volume

concentrations ranging from 0.2 to 0.8. The paper is limited to the estimation of heat transfer enhancement at different Reynolds number flowing through copper tube which subjected to constant heat flux boundary condition in the turbulent range at volume concentration of 0.02% with and without tape insert. The result gained is using twisted tape provide more enhancement in heat transfer compared to plain tubes even using the same flow rate.

Figure 2.8 shows the result of their data with 0.02% concentration in plain tube compare with values from (Park and Cho, 1998) equation for estimate plain tube with 0.02% concentration in plain tube. The experimental data has been put to regression having standard deviation of ± 0.3%, similar to the equation of (Sarma et al., 2003) valid in the laminar range of single phase fluids.

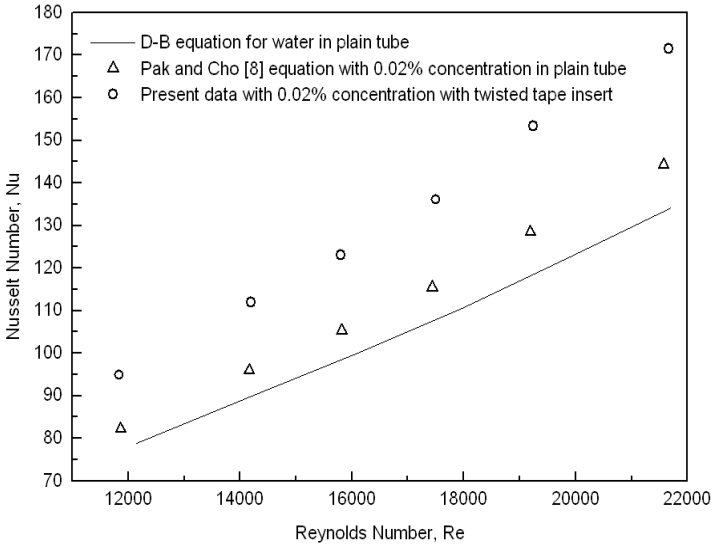

Figure 2.8: Nusselt number with and without twisted tape insert for nanofluid with 0.02% of concentration.

Source: (Sundar, L.S., et. al, 2007)

Researcher such as (Lee et al., 1999) and (Xuan and Li, 2000) stated that with low nanoparticles concentrations (1–5 %), the thermal conductivity of the suspensions can increase more than 20%. (Eastman et al.,1997) at Argonne National laboratory showed with some preliminary experiments with suspended nanoparticles, the thermal conductivity of approximately 60% can be obtained with volume concentration of 5 %

CuO nanoparticles in the based fluid of water. Heat transfer coefficient is the determining factor in forced convection cooling–heating applications of heat exchange equipments including engines and engine systems. Such enhancement mainly depends upon factors such as particle volume concentration, particle material, particle size, particle shape, base fluid material temperature, and additives.

(Das et al., 2000) examined the effect of temperature on thermal conductivity of nanofluids with water as a base fluid and particles of Al_2O_3 or CuO as suspension material. The results revealed that the thermal conductivity of nanofluids increased with temperature and the effective thermal conductivity models failed to predict the thermal conductivity of nanofluids. (Mansour et al., 1999) investigated the effect of uncertainties in physical properties for both fully developed laminar and turbulent forced convection in a tube with uniform heat flux at the wall.

There are several experimental and numerical studies about nanofluid convective heat transfer performance in laminar flow. A few numbers of studies have been carried out on nanofluid convective heat transfer performance in turbulent regime. Pak and Cho investigated the turbulent friction and heat transfer behavior of Al_2O_3/water and TiO2/water nanofluids in a circular pipe experimentally. Results showed that the convective heat transfer coefficient of nanofluids at a volume concentration of 3% was 12% smaller than that of pure water. This result was attributed to a significant increasing viscosity of nanofluids. They proposed the first empirical correlation for prediction of nanofluid Nusselt number in a turbulent flow.

(Xuan and Li, 2000) investigated flow and convective heat transfer characteristics for Cu/water based nanofluids through a straight tube with a constant heat flux at the wall experimentally. Results showed that nanofluids give substantial enhancement of heat transfer rate compared to pure water. They also claimed that the friction factor for the nanofluids at low volume fraction did not produce extra penalty in the pumping power.

(Williams and Buongiorno, 2002) examined the turbulent convective heat transfer behavior of alumina and zirconia nanoparticles dispersions in water in a

horizontal tube experimentally. They showed that the convective heat transfer coefficient can be predicted by means of the traditional correlations and observed no abnormal heat transfer enhancement.

(Fotukian and Nasr Esfahany, 1998) studied the convective heat transfer and pressure drop of dilute Al_2O_3/water nanofluid inside a circular tube under turbulent flow condition. Results indicated that the addition of small amounts of nanoparticles to the base fluid increased the heat transfer coefficient remarkably.

(Xuan and Roetzel, 2001) were the first to indicate a mechanism for heat transfer in nanofluids. They proposed thermal dispersion as a major mechanism of heat transfer in flowing fluid, along with the enhancement of nanofluid thermal conductivity. Results showed that the addition of nanoparticles can increase the heat transfer substantially compared to the base fluid. It was also found that the ethylene glycol-γAl_2O_3 provided better heat transfer enhancement than the water-γ Al_2O_3 nanofluids.

A new correlation was proposed by (Maiga et al., 1999) to describe the thermal performance of Al_2O_3/water nanofluids under turbulent regime. Buongiorno et al. conducted a numerical study of the turbulent heat transfer of nanofluids. The wall layer was considered to be consisted of a laminar sub layer and a turbulent core. The heat transfer enhancement was explained mainly by a reduction in viscosity within and consequent thinning of the laminar sub layer. It was also found that the Brownian diffusion and thermophoresis were the two most important nanoparticles/base-fluid slip mechanisms. Behzadmehr et al., (1998) applied a two phase mixture model to study the turbulent forced convection flow of Cu/water nanofluid with a volume fraction of 1.0% inside a uniformly heated tube numerically. Results also indicated that the nanofluid Nusselt number increased by more than 15% compared to base fluid.

(Heris et al., 1999) investigated convective heat transfer of nanofluids in a circular tube numerically and showed that heat transfer coefficients decreased with nanoparticles size. Ghasemi and Aminossadati investigated natural convection of nanofluid in an inclined enclosure. The influence of particle loading and inclination number was addressed. Our earlier work showed that addition of small amounts of

Al_2O_3 nanoparticles to water intensified heat transfer significantly but increasing the concentration of Al_2O_3 nanoparticles did not show a considerable effect.

(Sharma K.V et. al, 2009) have done an experiment of Convective heat transfer coefficient and friction factor data at various volume concentrations for flow in a plain tube and with twisted tape insert is determined experimentally for Al_2O_3 nanofluid. Experiments are conducted in the Reynolds number range of 10,000–22,000 with tapes of different twist ratios in the range of $0 < H/D < 83$. Figure 2.9 friction factor of 0.5% volume concentration of Al_2O_3 nanofluid with twist ratio of five is 33.51% and 1.096 times respectively higher compared to flow of water in a tube. A generalized regression equation is developed for the estimation of Nusselt number and friction factor valid for both water and nanofluid in plain tube and with inserts under turbulent flow conditions.

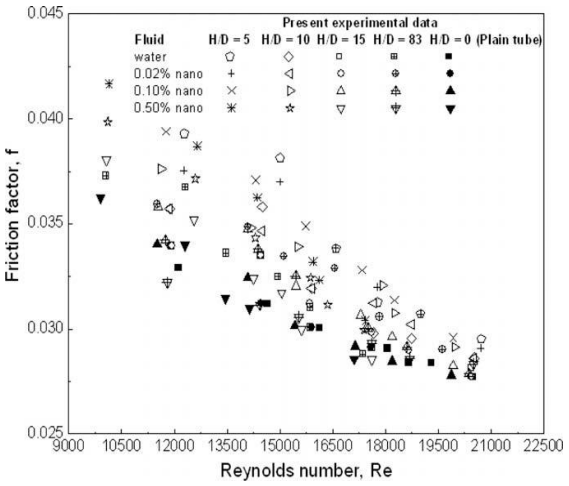

Figure 2.9: Experimental friction factor of water and nanofluid for flow in a tube and with tape insert

Source: (Sharma K.V et. al, 2009)

(Eiamsa-ard S., 2009) presents a paper of an experimental study on the mean Nusselt number; friction factor and enhancement efficiency characteristics in a round tube with short-length twisted tape insert under uniform wall heat flux boundary conditions. In the experiments, measured data are taken at Reynolds numbers in a turbulent region with air as the test fluid. The full-length twisted tape is inserted into the

tested tube at a single twist ratio of y/w=4.0 while the short-length tapes mounted at the entry test section are used at several tape length ratios 0.29, 0.43, 0.57 and 1.0 (full-length tape). The short-length tape is introduced as a swirling flow device for generating a strong swirl flow at the tube entry before decaying along the tube and the full-length tape (LR=1.0) is expected to produce a strongly swirling flow over the whole tube. The experimental result indicates that the short length tapes of LR=0.29, 0.43 and 0.57 perform lower heat transfer and friction factor values than the full-length tape around 14%, 9.5% and 6.7%; and 21%, 15.3% and 10.5%, respectively. In addition, it is apparent that the enhancement efficiency of the tube with the short-length tape insert is found to be lower than that with the full-length one. The mean deviation between measured and correlated values of the Nusselt number is in the order of ±7% in the range of Reynolds numbers from 4000 to 20,000.

(Shang S.W, 2009) proposed an experimental study that comparatively examined the two-phase flow structures, pressure drops and wall-to-fluid heat transfer properties between the plain tube and the enhanced tube with the spiky twisted-tape insert (swirl tube), was performed to disclose their differential thermal-fluid performances with air–water flows. On-line and post-processed high-speed digital images of air–water two-phase phenomena in plain and swirl tubes were detected to ensure the bubbly flow pattern in plain tube and to visualize their characteristic interfacial structures. Superficial liquid Reynolds number (*Re*) and air to water mass flow ratio (AW), which were respectively controlled in the ranges of 5000–15,000 and 0.0004–0.01, were selected as the controlling parameters of heat transfer performances. The dispersed rising air bubbles in the plain tube and the centrifugal-force induced coherent spiral stream of coalesced bubbles in the swirl-tube core considerably modify the pressure-drop and heat-transfer performances from the single-phase conditions. Selected results of pressure-drop and heat-transfer measurements, Flow images and tube-averaged void fractions detected from the plain and swirl tubes with air–water two-phase flows were cross-referenced to illustrate the mechanisms responsible for the modified thermal-fluid performance due to the spiky twisted-tape insert. Empirical heat transfer correlations which evaluate the Nusselt numbers over the developed flow regions of the plain and swirl tubes with air–water two-phase flows were generated for industrial applications.

Present experiments were performed in high concentrations of nanoparticles. Since this behavior rarely been reported, experiments with 0.5% of Al_2O_3 nanoparticles were planned to see if the same behavior was observed. Therefore, the aim of this study is to determine heat transfer coefficient of nanofluid inside a twisted circular tube in turbulent region. Table 2.1 present some of previous study related with research study.

Table 2.1: Summary of Experimental Investigations in Convective Heat Transfer

Experimental / Numerical	**Author**	**Working fluid**	**Condition**	**ϕ (%)**	**Flow Region**	**Result**
Experimental	Dongsheng et al. (2004)	Nanofluid (Al_2O_3)	Entrance Region	0 – 0.02	Laminar	Enhance HTC in Laminar as *Re* increased
Experimental and numerical	Sundar et al. (2007)	Nanofluid (Al_2O_3) and water	Without versus with twisted tape	0.02	Turbulent (10 000 - 22 000)	*Nu* for twisted tape higher than without and water
Experimental	Eiamsa-ard et al. (Feb 2009)	Water	Short-length twisted tape	-	Turbulent (4 000 – 20 000)	*Nu* increased for all twisted tape
Experimental and numerical	Sundar et al. (11th March 2009)	Nanofluid (Al_2O_3)	Circular tube and twisted tape (0<H/D<83)	0.02, 0.1, 0.5	Turbulent (10 000 – 22 000)	HTC with nanofluid and twisted tape higher than water
Experimental	Sharma et al. (25th March 2009)	Nanofluid (Al_2O_3) and water	Circular tube and twisted tape	0.1, 0.02	Transition	*Nu* for higher concentration is highest

CHAPTER 3

METHODOLOGY

3.1 INTRODUCTION

In chapter 3, the method used by the researcher for the experiment is being described in detail. Besides that, this chapter includes the flow of the research paper, information on preparation of nanofluid solution proposed by the researcher, the flow of experiment done using the suitable apparatus, and method of interpreting the result.

The experiment is suggested to vary in Reynolds number, volume concentration of nanofluid, several tape length ratios and type of nanoparticles. Reynolds number varies between 4 000 until 22 000 which shall be in turbulent region. On the other hands, nanofluid used is Alumina, Al_2O_3 with volume concentration of 0.5 % which is known as low volume concentration. The twist ratio, H/D used is 5, 10, 15 and 83. Occasionally, the twisted tape insert is known as passive disturbance for generating strong swirl flow along the test tube. Through the flow chart, experiment setup is clearly shown the research design. In order to achieve the objectives of this research paper, the suitable apparatus and experimental setup is needed. Thus, the collected data will be analyzed further and interpreted in suitable way to validate the data by compare with previous research and simulation paper.

3.2 FLOW CHART

Figure 3.1 shows the detail methodology throughout this research paper starting from research until the analysis based on the main objective line up for the study.

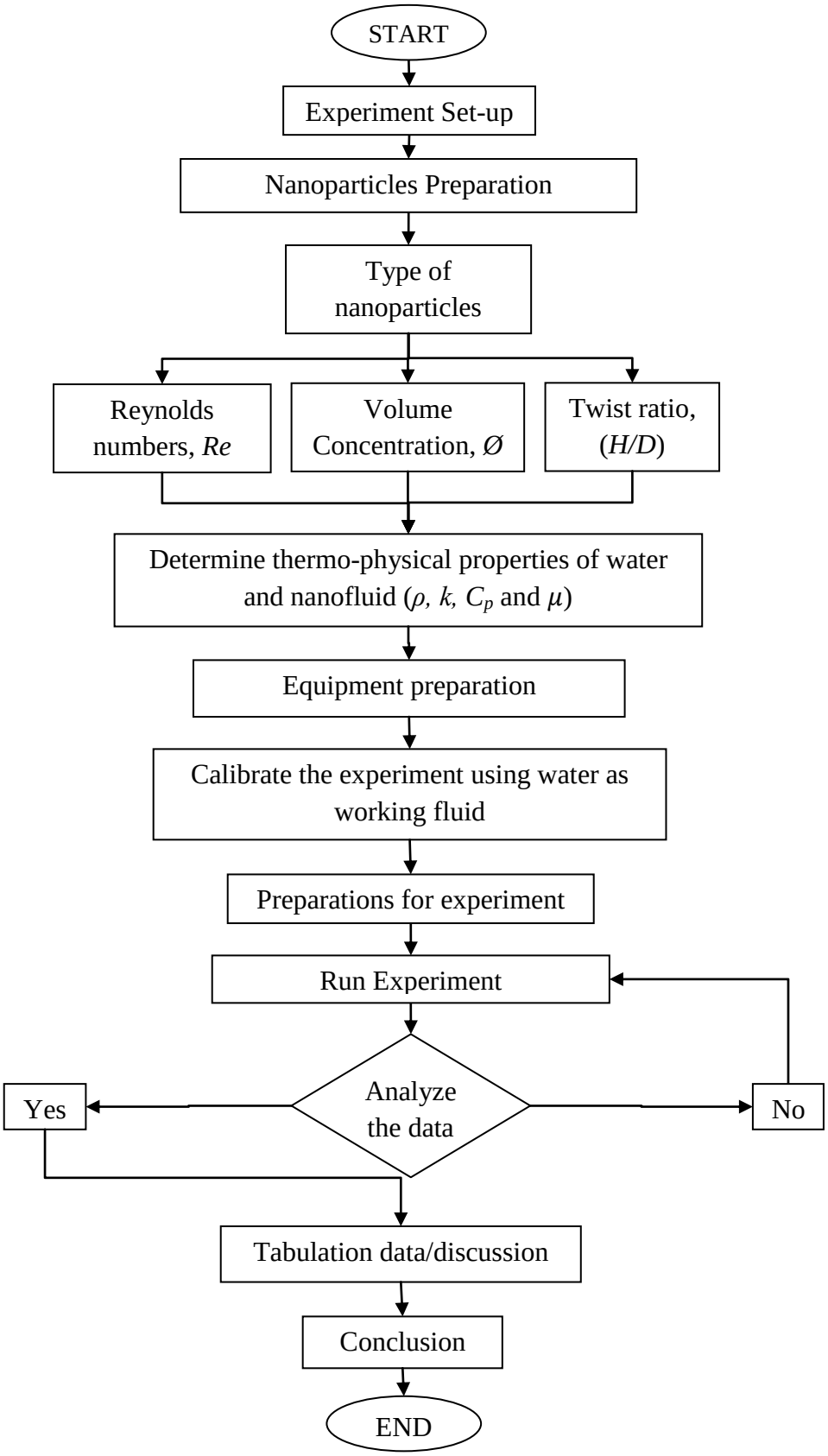

Figure 3.1: Flow diagram of the experiment

From Figure 3.1, the flow of the experiment can clearly be understood that the experiment starts with preparation of nanofluid at desired volume concentrations using two-step process. Secondly, the experiment is set up based on the schematic diagram and calibrated using water to check the consistency and the values is validate by comparing them with Dittus-Boelter equation and Gnielinski equation as in Eq. 2.14 and Eq. 2.15. If the values are not validate, the experiment set-up will be tested again and observer the causes. On the other hands, if the values are validate, the experiment will be continue using nanofluid after setting the variables that wants to be varies. Then, the experiment will be running and the required data will be taken and fills up in the tables at varies variable. Thus, the working fluid flow rate in the test section will be calculated based on totalizer readings and validated with manual measurements. By using Newton's law of Cooling, the experimental heat transfer coefficient is estimated. Before that, the properties of the fluid are considered at mean bulk temperature. Lastly, the data will be tabulated and compare with previous literature.

3.3 NANOPARTICLES PREPARATION

A meticulous preparation of nanofluid is a must as if the preparation is not right, then, the experiment will be wrong from the very beginning. Thus, by using the most commonly used technique of preparation which is two-step method, the nanoparticles which in dry powder condition are been prepared as nanofluid. The varies of Al_2O_3, CuO and TiO_2 with an average size of 47 nm are then dispersed with distilled water as the base fluid and small quantity of sodium dodecylbenzene sulfonate (SDBS) as dispersant to calculated amount of nanoparticles added. It is stirred for 12 hours continuously to provide uniform dispersion of nanoparticles in water. Figure 3.2 shows the prepared nanofluids with different concentration of 0.02%, 0.1%, and 0.5%. But, the experiment used 0.5% to simplify the experiment.

Figure 3.2: Prepared Nanofluid

3.4 THERMOPHYSICAL PROPERTIES

As an opening steps towards analysis process, determining the thermophysical properties for working fluid is a must step. For calibration process, properties for water is predicted using regression equation developed by Azmi (Azmi et al., 2010) as shown in Eq. 2.24 until 2.27 and verify with an saturated water properties table as in Appendix A. As for nanofluid, there is no established properties table, thus, the properties is predicted from by Azmi (Azmi et al., 2010) and Taufiq (Taufiq, 2010) as shown in Eq. 2.28 until 2.31 which verified using other established papers. From it, other related terms such as Reynolds number, Prandtl number, friction factor and lastly heat transfer coefficient can be determined.

3.5 CALIBRATION PROCESS

After the experimental set up is assembled, the storage tank is filled with the working fluid. Initial experiment is conducted with water to check consistency and the values are compared with equation of Dittus-Boelter and Gnielinski as in Eq. 2.14 and Eq. 2.15 to test the reliability of the setup. Through the close agreement between the raw data from the experiment and equation of Dittus-Boelter and Gnielinski, the real experiment will take place for further analysis.

3.6 EXPERIMENTAL SETUP

The experiment is setup following Figure 3.3 which based on Sharma, (2009) schematic diagram. The fluid flows through a copper tube with diameter of 0.019 m, a chiller, a reservoir tank with the help of pump. The test tube to be used in this research is copper tube with 1.5 m in length and 0.019 m in diameter. At the surface of the test section, it will be wrapped for 1.5 m using nichrome heaters of 1kW in order to have a uniform heat. Then this tube will be cooled by the working fluid through it applying convection heat transfer. The space between test section and outer casting will be insulated with rock wool in order to minimize heat loss to the atmosphere. The calibrated thermocouple in quantity of 5 will be used with 0.1˚C resolution. 3 of them will be located on the surface with the distance of 0.375, 0.75 and 1.125 m from inlet. The other 2 will be located at inlet and outlet for measuring the inlet and outlet temperature. These variables will be observed during the experiment. With the aid of a pump, the fluid is forced through the test section which connected to a storage tank. The storage tank with 30 liter is made of stainless steel. To allow the heated liquid in the test section to cool down, the fluid passed through the provided chiller. Using gravitational force effect, the liquid then flows to the storage tank. The provision of chiller aided in achieving steady state condition faster. It is assumed that heat conduction in the strip is negligible. Both side of the test section need 4mm holes to connect with the U-tube manometer. The storage tank is filled with the working fluid after the experimental set up is assembled. Initially, experiments are conducted with water followed by nanofluids to determine heat transfer coefficients for flow in a tube with twisted tape. Calibration process is conducted with water to check the consistency and the values compared with the equation of Dittus-Boelter and Gnielinski to test the reliability of the setup. Then the prepared nanofluids at volume concentrations of 0.5% are used and the detail procedure is elaborated in next section of 3.6. From the totalizer readings, the working fluid flow rate in the test section is calculated and validated with manual measurements. With the Newton’s law of cooling, the experimental heat transfer coefficient is estimated. The properties of the fluid are considered at the bulk or mean temperature. Required data at different flow Reynolds number range of 10,000–22,000 are recorded with flow of water and nanofluid in a tube with twisted tape for heat transfer coefficient estimation and relevant comparisons made.

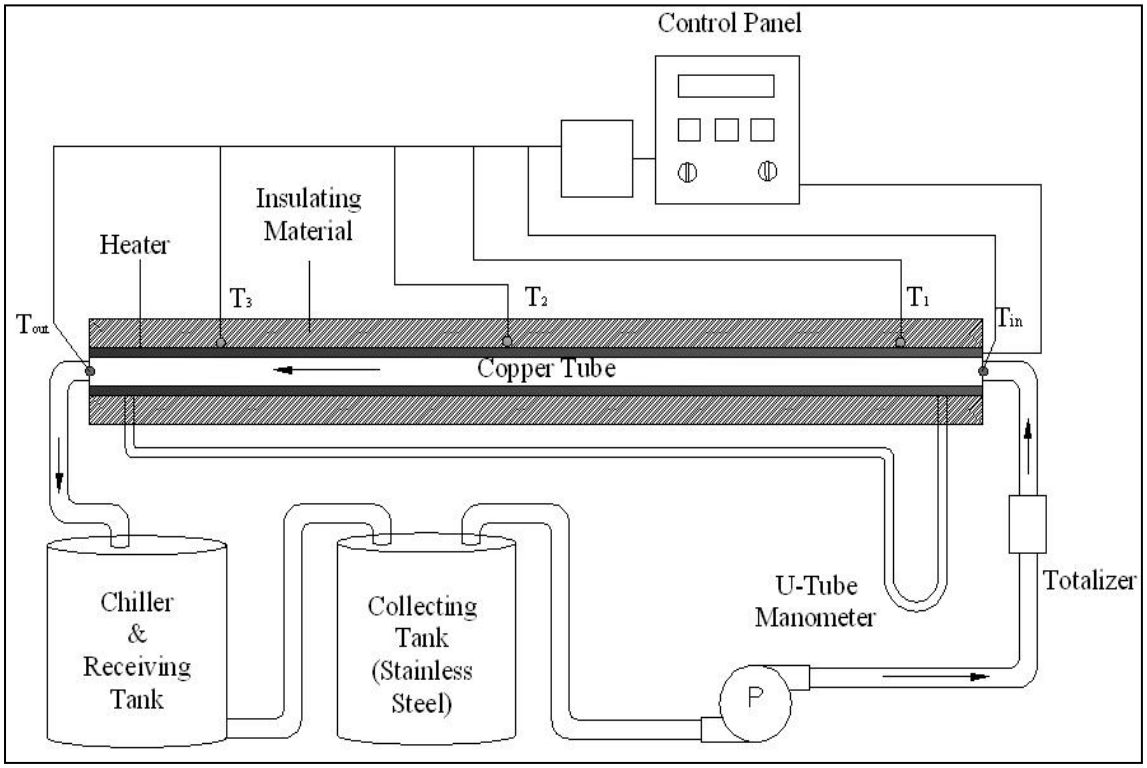

Figure 3.3: Schematic Diagram Experimental Setup

Source : Sundar et al., (2009).

The twisted tape used throughout the experiment has 1 mm of thickness and 0.018 m of width. The strip prepared by the researcher to be used is made of aluminum as shown in Figure 3.4.

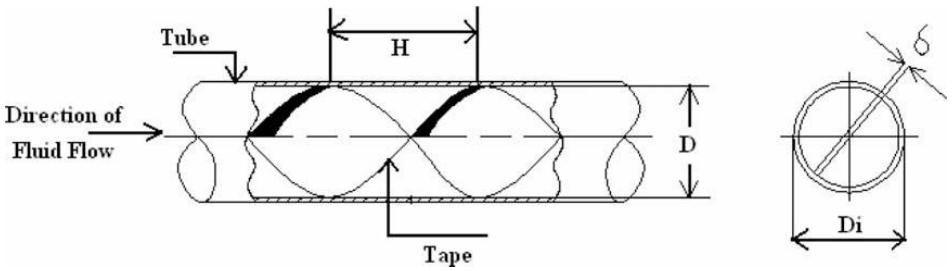

Figure 3.4: Full-length twisted tape insert inside a tube

Source : Sundar et al., (2009)

For the dimensions of twisted tapes are given in Table 3.2. Whereas, by subjecting both ends of the strip to lathe machine, one at the headstock end while another one at the tail stock end. The strip is then twisted manually by turning the chuck to obtain twist ratio of 5, 10, 15 and 83. The twisted tape ratio is one of variable that will be varies along in this research. By assuming that heat conduction in the strip is negligible.

Table 3.1: Dimensions of the twisted tape inserts

S. No.	**Parameter**	**Twist ratio, H/D (m)**			
		5	10	15	83
1	H (width)	0.09	0.18	0.27	1.5
2	D (diameter)	0.018	0.018	0.018	0.018

Source: Sundar et al., (2009)

3.7 EXPERIMENT APPARATUS

The experiment apparatus to estimate the heat transfer coefficient of the nanofluid which flowing in a tube with twisted tape has been fabricated as shown in Figure 3.5. It consists of a chiller, reservoir tank, pump, totalizer, copper tube with thermocouples for temperature measurement, control panel and U-tube manometer. Table 3.2 shows the summary of experiment apparatus used.

Notation:

[1] Chiller
[2] Reservoir Tank
[3] Pump
[4] Totalizer
[5] Copper Tube
[6] Control Panel
[7] U-tubemanometer
[8] Thermocouple

Figure 3.5: Fabricated experiment apparatus

Provided chiller used to cool down the heated liquid as shown in Figure 3.6. In addition, the chiller is helped nanofluid to achieve steady state condition faster. The reservoir tank or also known as storage tank is used as the storage tank with aid of a variable pump. The storage tank as in Figure 3.7 is made of stainless steel with capacity of 30 liter. A variable pump is used as urging force to flow though the test section. The suction side connected to a storage tank is shown in Figure 3.8. Figure 3.9 showing a totalizer or flow rate controller used as controller of fluid flow.

Figure 3.6: Chiller

Figure 3.7: Reservoir Tank

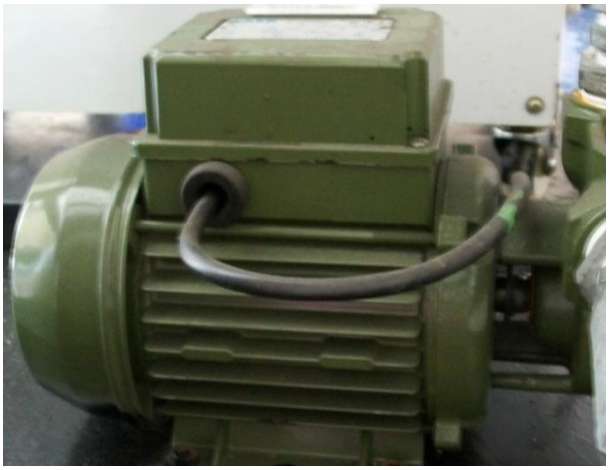

Figure 3.8: Pump

Figure 3.9: Totalizer

Copper tube is used as the test section and wrapped with two nichrome heaters of 20 gauges, having a resistance of 53.5 Ω per meter length and 1000 W maximum rating. Along the test section, constant heat flux boundary condition is set up. Figure 3.10 (a) and Figure 3.10 (b) show a clearer view of the front and back of the test section

whereas Figure 3.10 (c) shows a pair of thermocouple and heater attached to the test tube.

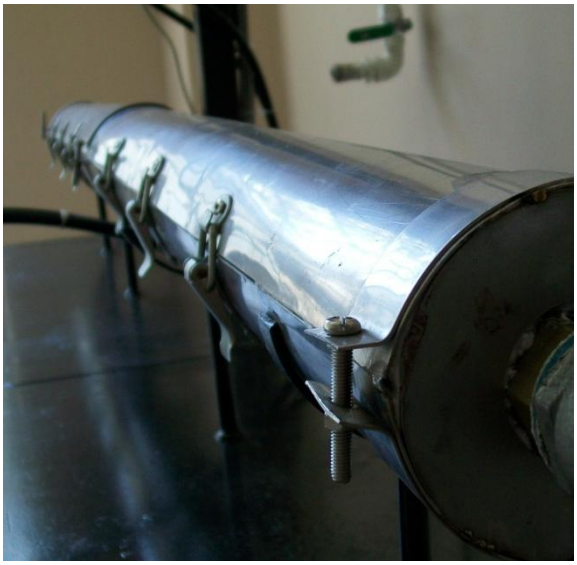

(a) Front view of test section

(b) Back view of test section with heaters and thermocouples

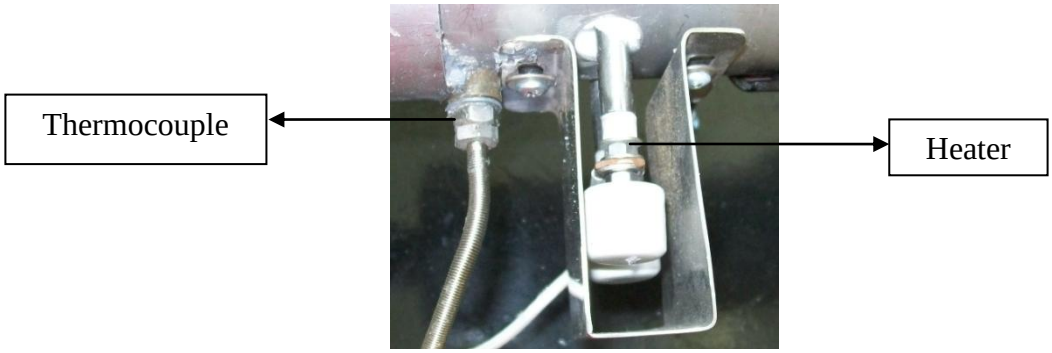

(c) Top view of heater and thermocouple attached to test section

Figure 3.10 (a), (b) & (c): Copper tube (Test section attached with heater and thermocouple)

Control panel is used to monitor temperatures along the test section and shown in Figure 3.11. The panel contains digital reading for 5 specify points of thermocouples attached to the test section. Figure 3.12 is U-tubemanometer used as measurement of pressure drop at different Reynolds number. The manometric liquid used for determining the pressure drop at different flow rates is Carbon tetrachloride. Twisted tape is used as the passive disturbance for the fluid flow. To allow hydrodynamic flow

is developed, the aspect ratio of the test section is sufficiently large. Figure 3.13 showing twisted tape used in the experiment.

Figure 3.11: Control Panel

Figure 3.12: U-tube manometer

Figure 3.13 : Twisted tape insert

Table 3.2: Summary of materials and equipments required for the experiment

Material/Equipment	**Description**
Nanofluid: Al_2O_3, CuO and TiO_2	Al_2O_3, CuO and TiO_2 are use as the working fluid that will be carrier for the thermal heat from the test section. The working fluid will be cooled by chiller.
Copper tube	Copper tube with 1.5 m in length and 0.019m in diameter.

Table 3.2: Continued

Material/Equipment	Description
Collecting Tank	The tank is stainless steel wit capacity of 301.
Thermocouple	5 calibrated thermocouples will be used with 0.1˚C resolution.
Flow meter	The flow rate of working fluid in the test section will be determine by the flow meter
U-tube manometer with fluid of carbon tetrachloride	The manometer will take the pressure drop across the test section.
Pump	The pump will circulate the working fluid.

3.8 EXPERIMENTAL PROCEDURES

After the experimental set up has been prepared and calibrated, to proceed with the experiment, the procedures are as follows:

i. Prepare all the apparatus needed and make sure experiment setup already done.
ii. The experiment setup is firstly calibrated using water as working fluid. After the value is checked as consistence, next experiment is using the interest working fluid.
iii. Before get start, the working fluid of nanofluid is fill-in the tank.

iv. For the first tempt, using volume concentration 0.5% Al_2O_3 nanofluid with flow rate of 0.18 L/s. At the same time, start heat up the copper tube with inserted tape of 5 twist ratio using nichrome heater of 1kW.
v. When the copper tube already at 100^oC, the working fluid is left to circulate through the loop using variable speed of pump suitable capacity.
vi. After the system attains steady state, measure the temperature at 5 point start at inlet, T1, T2, T3 and outlet.
vii. Change the twist ratio to 10, 15 and 83 and take the measured data.
viii. Repeat procedure 4 until 7 by using 12 different flow rates.
ix. Take the data measured and fill into the table.
x. With help of assumptions, the measured data will be analyzed to estimate the convection heat transfer coefficient.
xi. The data will be presented in suitable graph to validate the data by compare with previous experiment and simulation paper.

3.9 EXPERIMENT PROCESS FLOW

Figure 3.14 is provided to deeper understanding of the experiment process flow starting with circulates the working fluid using pump and ends with cooling down working fluid. Further explanation as follows:

i. Part 1: The pump will circulate the working fluid with the flow rate adjusted by the researcher.
ii. Part 2: Working fluid temperature will be increasing as heat transfer occurs in the system. Temperature after the working fluid flows through the test tube is taken at five (5) different points on test tube.
iii. Part 3: The working fluid carries out the heat and cooled down in the chiller about 15 seconds.
iv. Part 4: The cooled working fluid is collected in the tank before it can use again to circulate in the experimental set up.

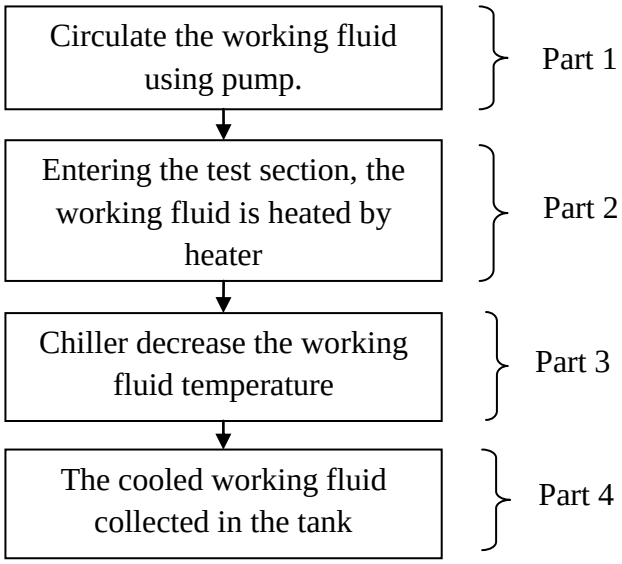

Figure 3.14: Experiment process flow

3.10 ANALYSIS OF EXPERIMENTAL DATA

After finished run the experiment, analysis of experimental data takes place in order to obtain HTC value for nanofluid. Detailed explanation regarding the analysis is explained in the following subchapter.

3.10.1 Reynolds Number

Throughout the experiment, the condition for the experiment is assume to have no heat loss to environment in order to applied Newton's Cooling law as discussed in previous subchapter 2.8.2. Hence, Reynolds number is rearranged to match the available data and calculated using Eq. 2.18 as follow:

$$Re = \frac{4\dot{m}}{\pi D_i \mu} \tag{3.1}$$

Where $\dot{m}$ is mass flow rate, D_i is inner diameter tube and μ is dynamic viscosity of the working fluid.

3.10.2 Experimental Heat Transfer Coefficient

From rearranged Newton's law of cooling in Eq. 2.17, HTC experiment, h is calculated as follow:

$$h_{exp} = \frac{\dot{Q}}{A_s (T_w - T_b)_{avg}} \tag{3.2}$$

$\dot{Q}$ is the energy supplied from the heater which could be calculated using Eq. 3.3 or Eq. 3.4. V is voltage supplied to the heater and I is the current supplied to the heater.

$$\dot{Q} = V \times I \ \left(energy\ supplied\right) \tag{3.3}$$

$$= \dot{m} C_P \left(T_e - T_i\right) \tag{3.4}$$

T_w is the average of total temperature readings for thermocouples at each point and bulk temperature, T_b is taken as average temperature of inlet temperature, T_i and outlet temperature T_e.

$$T_{w(avg)} = \frac{T_1 + T_2 + T_3}{3} \tag{3.5}$$

$$T_b = \frac{T_i + T_e}{2} \tag{3.6}$$

3.10.3 Experimental Nusselt Number

For experiment Nusselt number, it is calculate from Eq. 2.22. Based on the equation, when Nusselt number is higher, value of HTC is high which represent very good heat transfer.

$$Nu_{\exp} = \frac{hD_i}{k}$$

CHAPTER 4

RESULTS AND DISCUSSION

4.1 INTRODUCTION

Through this chapter, clear presentations of full analysis for experimental data are provided and further discuss. With nanofluid Al_2O_3 of volume concentration 0.5% as the working fluid, the analysis focus on the effect of using different twisted ratio. The twist ratio, H/D used is 5, 10, 15 and 83. Earlier, the properties for the working fluid is determine using regression equation and verified the values using either from established properties table or other established equation.

Next, calibration analysis using water is done in order to check the consistency of the apparatus before proceed with experiment using nanofluid. Thus, each finding are analyzed by using appropriate equation in order to evaluate heat transfer coefficient, h; Reynolds number, Re; Prandtl number, Pr and Nusselt number, Nu. The collected result data is present in graph of Nusselt number versus Reynolds number and discusses the pattern by comparing it with Gnielinski equation using water.

4.2 THERMOPHYSICAL PROPERTIES STUDY

Before analyzing the data, thermophysical properties for each data are need to be determine using regression equation from other research paper. Since the properties of working fluid is also consider as dependent factor for the analysis, hence, the regression equation need to be verified. Obviously, the properties for water is differ than properties of nanofluid.

4.2.1 Regression Properties for Water

Water is used as working fluid for the calibration analysis. The properties used for the analysis are density, specific heat, thermal conductivity and viscosity. Thus, water properties is determine using regression equation developed by Azmi (Azmi et al., 2010) as shown in Eq. 2.22 until 2.25. Then, properties data was compared with established properties of saturated water in Appendix A and presented in Table 4.1.

Table 4.1: Thermophysical Properties Data distribution

	Bulk Temperature, T_b (˚C)	**Density, ρ (Kg/m^3)**	**Specific Heat, C_p (J/Kg.K)**	**Thermal Conductivity, k (W/m.K)**	**Dynamic Viscosity, μ 10^{-3} (Kg/ms)**
Properties of Saturated Water (Appendix A)	30.0	996.00	4178.0	0.6150	0.798
	32.5	995.00	4178.0	0.6190	0.759
	35.0	994.00	4178.0	0.6230	0.720
	37.5	993.05	4178.5	0.6270	0.687
	40.0	992.10	4179.0	0.6310	0.653
	42.5	991.10	4179.5	0.6340	0.625
Regression Equation (Azmi et al., 2010)	30.0	995.68	4178.26	0.6150	0.800
	32.5	994.90	4177.98	0.6190	0.755
	35.0	994.06	4177.93	0.6229	0.714
	37.5	993.18	4178.05	0.6266	0.676
	40.0	992.25	4178.34	0.6303	0.641
	42.5	991.27	4178.75	0.6338	0.610

Through Figure 4.1 to 4.4, the water properties was plotted with intention of comparing them with properties of saturated data and found to have close agreement between them with average deviation less than 1.1 %. This proves that Regression equation by Azmi et al. (2010) is valid to predict thermophysical properties of water.

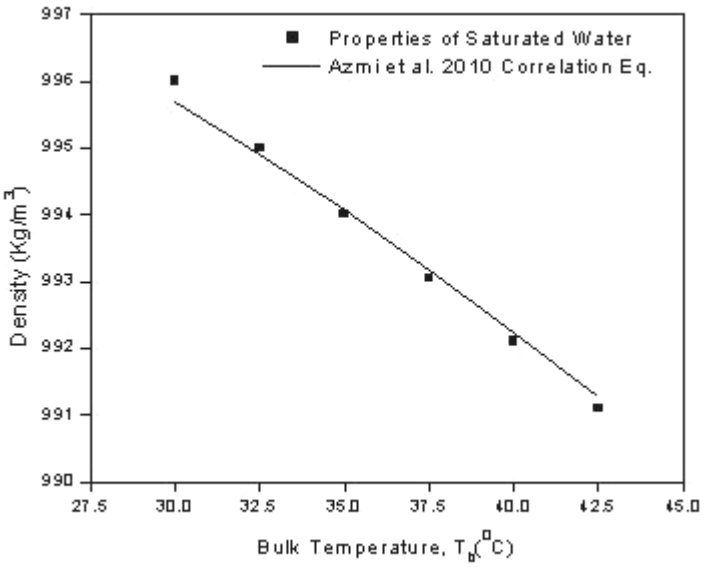

Figure 4.1: Comparison of Density between Properties Saturated Water and Correlation Equation by Azmi et al. (2010)

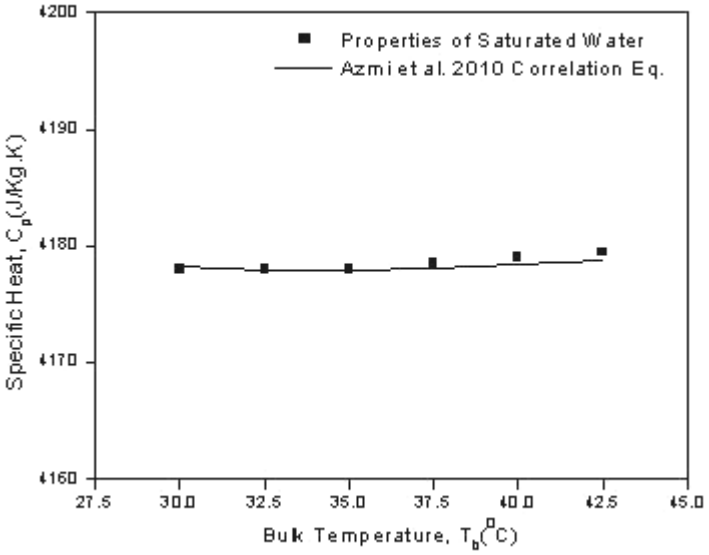

Figure 4.2: Comparison of Specific Heat between Properties Saturated Water and Correlation Equation by Azmi et al. (2010)

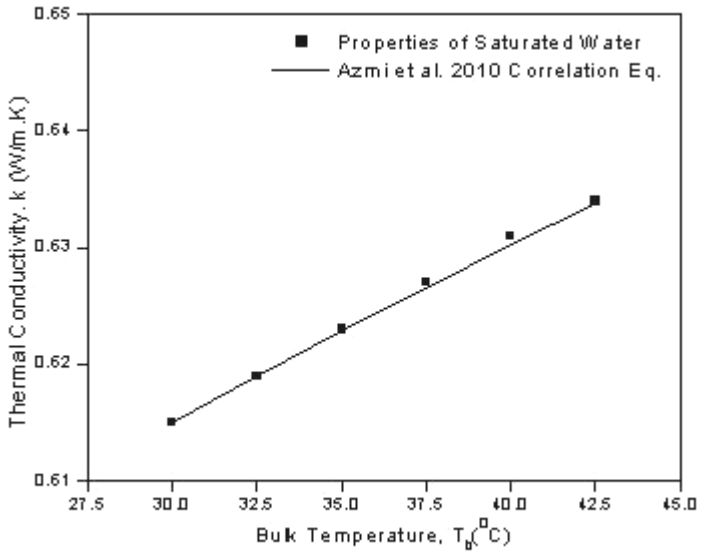

Figure 4.3: Comparison of Thermal Conductivity between Properties Saturated Water and Correlation Equation by Azmi et al. (2010)

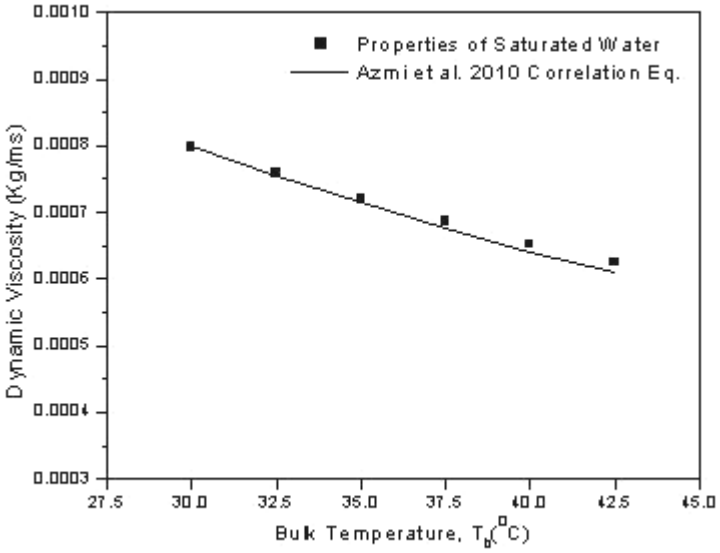

Figure 4.4: Comparison of Dynamic Viscosity between Properties Saturated Water and Correlation Equation by Azmi et al. (2010)

4.2.2 Regression Properties for Nanofluid

For the research experiment, Alumina, Al_2O_3 is used as working fluid. The properties used for the analysis are density, specific heat, thermal conductivity and viscosity. Thus, nanofluid properties is determine using regression equation developed by Azmi (Azmi et al., 2010) and Taufiq (Taufiq, 2010) as shown in Eq. 2.27 until 2.30. Since there is no established properties table for nanofluid and the properties does influence the analysis, the regression equation is verified based on other established papers in Figure 4.5 until 4.8. By comparison, the regression equation is found to have close agreement between other established equations with average deviation less than 10 %. This proves that Regression equation by Azmi and Taufiq is valid to predict thermophysical properties of water.

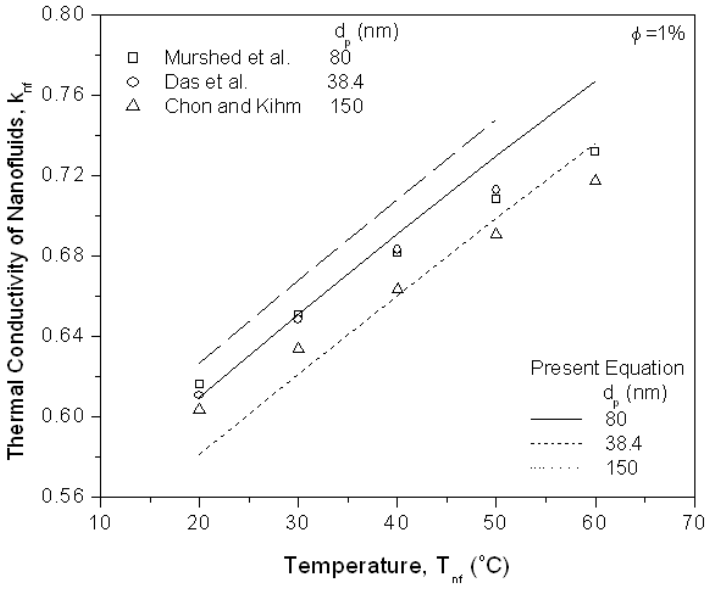

Figure 4.5: Comparison between regression equation and experiment data for thermal conductivity

Source: Azmi et al. (2010)

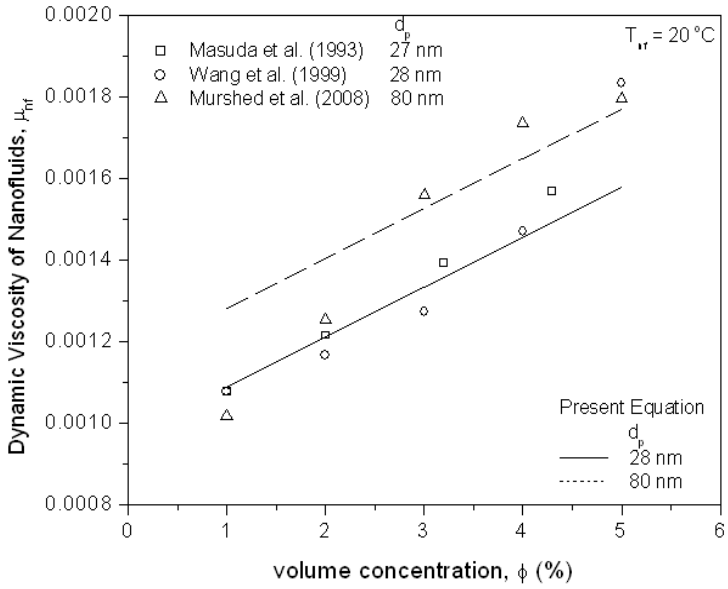

Figure 4.6: Comparison between regression equation and experiment data for dynamic viscosity

Source: Azmi et al. (2010)

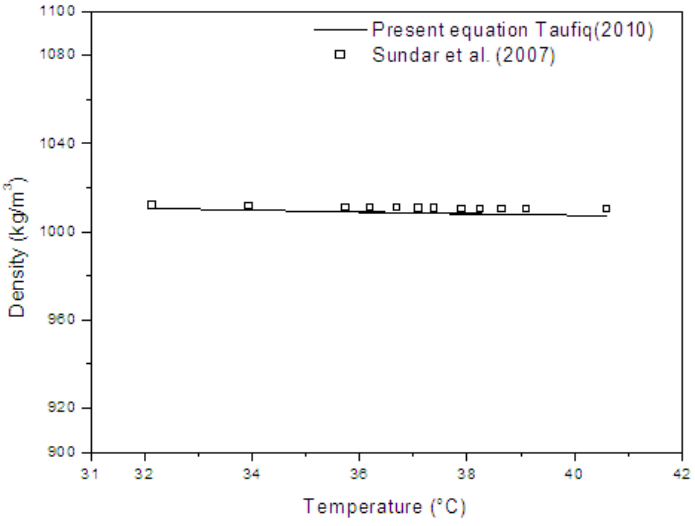

Figure 4.7: Comparison between regression equation and experiment data for density

Source: Taufiq (2010)

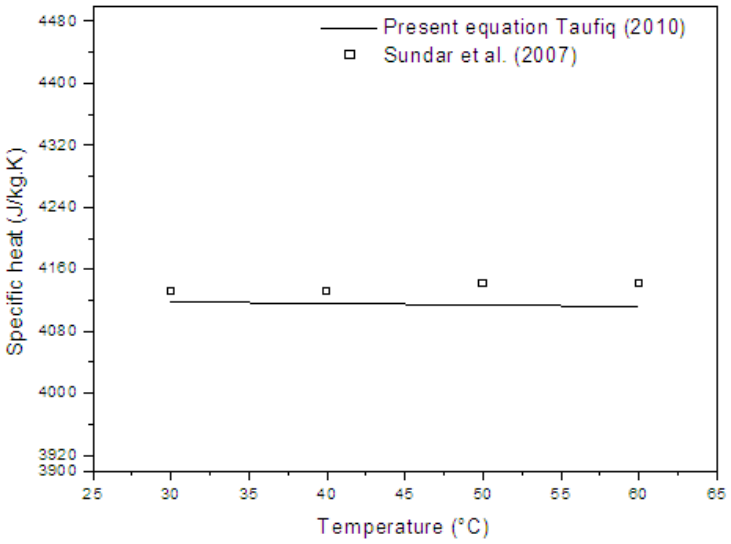

Figure 4.8: Comparison between regression equation and experiment data for specific heat

Source: Taufiq (2010)

4.3 CALIBRATION ANALYSIS

In order to check the apparatus consistency, initial experiment using water as working fluid in a plain tube in a range of Reynolds number has been done by running the experiment at 12 different flow rates. By using FORTRAN, the crude experimental data for water is transform to actual value. Next, actual values of experiment were compared with the calculated values using Gnielinski Eq. (Gnielinski, 1976) and Dittus-Boelter Eq. (Dittus-Boelter, 1930).

Calibration result obtained using water as working fluid is provided in Table 4.2. V_{avg} is obtained from totalizer readings, Bulk temperature and average wall temperature are calculated using Eq. 3.5 and 3.6.

Table 4.2: Temperature distribution for water in plain tube

No.	V_{avg} (Liter/sec)	T_{bulk} (˚C)	`T_{wall} (˚C)
1	0.18	39.7	73.0
2	0.23	38.4	71.0
3	0.28	37.5	69.0
4	0.33	36.4	67.0
5	0.38	35.5	65.4
6	0.45	34.9	62.8
7	0.52	37.7	67.3
8	0.64	37.0	62.6
9	0.72	36.5	59.9
10	0.81	35.4	56.6
11	0.94	33.2	52.4
12	1.12	31.3	48.9

Using water as the working fluid, Table 4.3 showed the calculation distribution of mass flow rate, $\dot{m}$, Darcy friction factor, *f*, Prandtl number, Pr, Reynolds number, *Re* and heat transfer coefficient, *h*. Nusselt number calculated using Dittus-Boelter equation from Eq. 2.14.

Table 4.3: Data distribution using Dittus-Boelter Eq.

No.	$\dot{m}$	*f*	*Pr*	*Re*	*h*	$Nu_{water,dittus-boelter}$
1	0.03647	0.011828	4.2899	3779.4	993.38	29.97
2	0.04638	0.011010	4.4259	4673.0	1188.29	35.96
3	0.05641	0.010392	4.5206	5576.1	1377.45	41.77
4	0.06573	0.009973	4.6409	6345.5	1539.59	46.81
5	0.07630	0.009577	4.7431	7222.8	1718.86	52.37
6	0.08966	0.009150	4.8073	8385.4	1944.67	59.33
7	0.10445	0.008590	4.4993	10368.9	2259.34	68.48
8	0.12726	0.008148	4.5747	12445.6	2627.68	79.78
9	0.14325	0.007902	4.6242	13874.1	2875.60	87.40
10	0.16256	0.007681	4.7547	15354.7	3144.75	95.84
11	0.18889	0.007468	5.0141	17008.6	3467.77	106.25
12	0.22495	0.007209	5.2680	19376.1	3906.20	120.28

By using water as the working fluid, Table 4.4 showed the calculation distribution of mass flow rate, $\dot{m}$, Darcy friction factor, *f*, Prandtl number, Pr, Reynolds

number, *Re* and heat transfer coefficient, *h*. Nusselt number calculated using Gnielinski equation from Eq. 2.15.

Table 4.4: Data distribution using Gnielinski Eq.

No.	$\dot{m}$	*f*	*Pr*	*Re*	*h*	$Nu_{water,gnielinski}$
1	0.03647	0.011828	4.2899	3779.4	898.36	27.10
2	0.04638	0.011010	4.4259	4673.0	1138.38	34.45
3	0.05641	0.010392	4.5206	5576.1	1369.96	41.54
4	0.06573	0.009973	4.6409	6345.5	1565.81	47.61
5	0.07630	0.009577	4.7431	7222.8	1782.61	54.32
6	0.08966	0.009150	4.8073	8385.4	2057.21	62.77
7	0.10445	0.008590	4.4993	10368.9	2451.97	74.32
8	0.12726	0.008148	4.5747	12445.6	2899.55	88.03
9	0.14325	0.007902	4.6242	13874.1	3201.22	97.30
10	0.16256	0.007681	4.7547	15354.7	3527.22	107.50
11	0.18889	0.007468	5.0141	17008.6	3916.99	120.02
12	0.22495	0.007209	5.2680	19376.1	4451.02	137.06

By using water as the working fluid, Table 4.3 showed the calculation distribution of mass flow rate, $\dot{m}$, Darcy friction factor, *f*, Prandtl number, Pr, Reynolds number, *Re* and heat transfer coefficient, *h*. Nusselt number for experiment is calculated using the calibration data where have been discussed in previous subchapter, 3.10.3.

Table 4.5: Data distribution of experiment for water in plain tube

V = 190V ; I = 3 A `						
No.	$\dot{m}$	V_{avg}	*Re*	*h*	$Nu_{w,theory}$	$Nu_{w,exp}$
1	0.03647	0.18	3779.4	30.19	30.17	30.17
2	0.04638	0.23	4673.0	34.77	34.78	34.78
3	0.05641	0.28	5576.1	39.43	39.44	39.44
4	0.06573	0.33	6345.5	43.46	43.47	43.47
5	0.07630	0.38	7222.8	47.62	47.62	47.62
6	0.08966	0.45	8385.4	53.14	53.11	53.11
7	0.10445	0.52	10368.9	71.38	71.42	71.42
8	0.12726	0.64	12445.6	81.30	81.34	81.34
9	0.14325	0.72	13874.1	88.47	88.44	88.44
10	0.16256	0.81	15354.7	97.02	97.03	97.03
11	0.18889	0.94	17008.6	107.31	107.32	107.32
12	0.22495	1.12	19376.1	116.24	116.20	116.20

Using actual values, Nusselt number of experiment is calculated and compared in Figure 4.9. From the plotted graph, it is shown that there is a close agreement between the experimental results of Nusselt number and the calculated values obtained from Gnielinski Eq. and Dittus-Boelter Eq. with average of deviation of 1.1% and 1.7%.

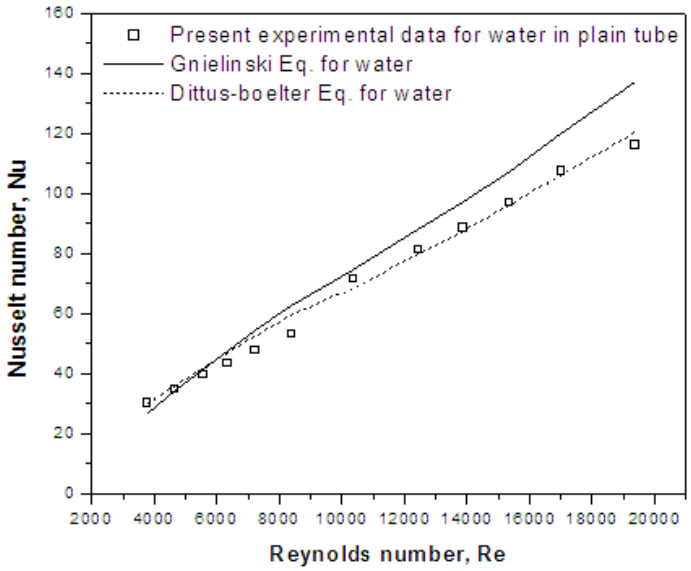

Figure 4.9: Comparison of experimental data of water with Gnielinski Eq. and Dittus-boelter Eq.

Nusselt number for experiment versus Nusselt number from Gnielinski was plotted as in Figure 4.10 shows the mean deviation between measured and correlated values of the Nusselt number is in the order of ±10% in the range of Reynolds numbers from 4000 to 20,000. Therefore, the apparatus is reliable to conduct the experiment.

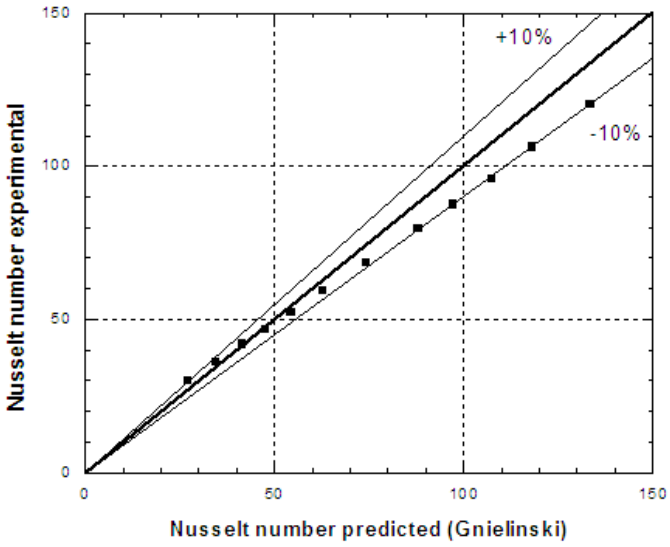

Figure 4.10: Nusselt number comparison for water

4.4 EXPERIMENTAL RESULT OF NANOFLUID

The test result of Alumina nanofluid, Al_2O_3 for the experiments is presented in Tables 3.4 to 3.8 with volume concentration, ϕ of 0.5 %. The twist ratio, *H/D* used is 5, 10, 15 and 83 for each flow rate. By using FORTRAN, the crude experimental data for nanofluid is transform to actual value. Results for experiments are further discussed in next subchapter.

4.4.1 For Al_2O_3 with Volume concentration, ϕ = 0.5%; Twist ratio, *H/D* = 5;

Experimental result obtained using nanofluid as working fluid twist ratio of 5 is provided in Table 4.6. V_{avg} is obtained from totalizer readings, Bulk temperature and average wall temperature are calculated using Eq. 3.5 and 3.6. The sample calculation for thermo-physical properties, mass flow rate, $\dot{m}$, heat transfer coefficient, *h* and Nusselt number, *Nu* are shown in APPENDIX B.

Table 4.6: Temperature distribution for Al_2O_3 with Volume concentration, ϕ = 0.5%; Twist ratio, *H/D* = 5;

No.	V_{avg} (Liter/sec)	T_{bulk} (˚C)	`T_{wall} (˚C)
1	0.16	40.2	68.7
2	0.21	38.7	65.6
3	0.25	37.7	64.1
4	0.31	36.6	62.0
5	0.35	35.7	60.6
6	0.40	35.3	58.8
7	0.55	38.0	59.7
8	0.68	37.3	58.1
9	0.75	36.8	56.6
10	0.90	35.8	54.2
11	0.96	33.4	50.4
12	1.09	31.6	48.2

Table 4.7 showing the calculation distribution of mass flow rate, $\dot{m}$, Darcy friction factor, *f*, Prandtl number, *Pr*, Reynolds number, *Re* and heat transfer coefficient, *h*. Nusselt number for experiment is calculated using the experimental data where have been discussed in previous subchapter, 3.10.3.

Table 4.7: Data distribution of experiment for Al_2O_3 with Volume concentration, ϕ = 0.5%; Twist ratio, *H/D* = 5;

V = 190V ; I = 3 A `						
No.	$\dot{m}$	V_{avg}	***Re***	***h***	$Nu_{w,theory}$	$Nu_{w,exp}$
1	0.03647	0.16	3248.4	1159.30	30.03	31.42
2	0.04644	0.21	4014.1	1514.06	37.81	41.38
3	0.05640	0.25	4773.3	1617.56	40.99	44.47
4	0.06970	0.31	5761.6	1892.07	47.56	52.36
5	0.07968	0.35	6459.2	2038.75	51.51	56.72
6	0.08965	0.40	7196.2	2237.14	57.59	62.41
7	0.12272	0.55	10441.3	2703.47	60.11	74.22
8	0.15266	0.68	12796.7	2782.53	68.49	76.70
9	0.16924	0.75	14050.3	3100.93	79.88	85.71
10	0.20245	0.90	16447.4	3259.13	85.91	90.62
11	0.21589	0.96	16632.1	3899.39	105.69	110.00
12	0.24589	1.09	18185.8	4154.89	119.86	118.51

Experimental Nusselt number for nanofluid of Al_2O_3 flow in a tube with twist ratio, *H/D* of 5 is presented in Figure 4.11. The figure shows increasing value of Nusselt number for nanofluid Al_2O_3 with twist ratio, *H/D* of 5 and water in plain tube to be compared. In low range of Reynolds number, Re, nanofluid have greater value of Nusselt number than water in plain tube. After Reynolds number of 12000, water in plain tube have greater value of nanofluid. This due to unstable flow and the flow are not cooled down enough.

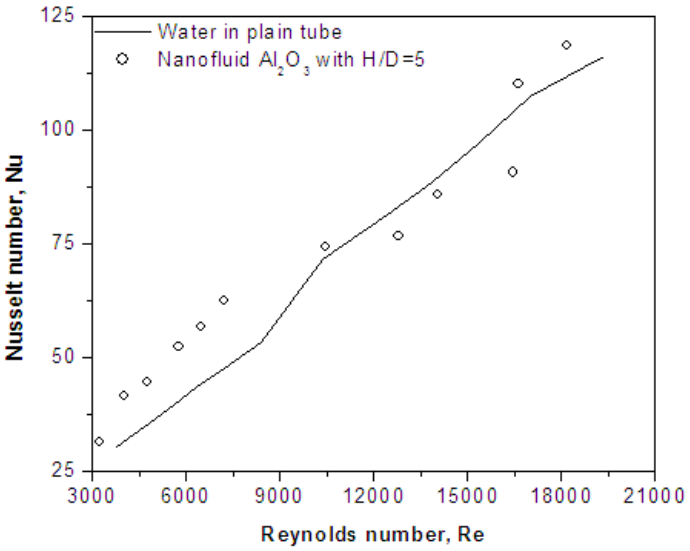

Figure 4.11: Nusselt number versus Reynolds number for nanofluid with *H/D* = 5

4.4.2 For Al_2O_3 with Volume concentration, ϕ = 0.5%; Twist ratio, *H/D* = 10;

Next, using nanofluid as working fluid with twist ratio of 10 experimental result obtained is provided in Table 4.8. V_{avg} is obtained from totalizer readings, Bulk temperature and average wall temperature are calculated using Eq. 3.5 and 3.6. The experiments are run for 12 time at different flow rate.

Table 4.8: Temperature distribution for Al_2O_3 with Volume concentration, ϕ = 0.5%; Twist ratio, *H/D* = 10;

No.	V_{avg} (Liter/sec)	T_{bulk} (˚C)	`T_{wall} (˚C)
1	0.17	40.4	65.5
2	0.21	39.1	62.6
3	0.26	38.1	60.6
4	0.32	37.0	58.7
5	0.36	36.1	56.8
6	0.43	35.7	56.1
7	0.56	38.5	55.9
8	0.71	37.8	54.0
9	0.81	37.3	52.6
10	0.92	36.5	51.4
11	1.00	33.8	48.2
12	1.10	32.1	45.8

Table 4.9 showing the calculation distribution of mass flow rate, $\dot{m}$, Darcy friction factor, *f*, Prandtl number, *Pr*, Reynolds number, *Re* and heat transfer coefficient, *h*. Nusselt number for experiment is calculated using the experimental data where have been discussed in previous subchapter, 3.10.3. The data di

Table 4.9: Data distribution of experiment for Al_2O_3 with Volume concentration, ϕ = 0.5%; Twist ratio, *H/D* = 10;

V = 190V ; I = 3 A `						
No.	$\dot{m}$	V_{avg}	***Re***	***h***	$Nu_{w,theory}$	$Nu_{w,exp}$
1	0.03703	0.17	3315.0	1371.90	31.16	37.13
2	0.04713	0.21	4103.9	1673.21	36.58	45.64
3	0.05726	0.26	4887.1	1894.42	41.03	51.96
4	0.07075	0.32	5898.9	2235.38	48.08	61.71
5	0.08087	0.36	6613.0	2468.67	52.01	68.52
6	0.09772	0.43	7913.3	2706.83	60.43	75.33
7	0.12456	0.56	10721.6	3250.74	57.93	88.96
8	0.15823	0.71	13406.0	3660.09	70.48	100.60
9	0.18191	0.81	15248.3	4026.04	80.28	110.98
10	0.20548	0.92	16949.1	4037.47	86.37	111.79
11	0.22574	1.00	17547.3	4472.40	102.68	125.86
12	0.24953	1.10	18645.4	4756.08	113.92	135.28

Experimental Nusselt number for nanofluid of Al_2O_3 flow in a tube with twist ratio, *H/D* of 10 is presented in Figure 4.12 below. Beautiful increasing values of Nusselt number for nanofluid Al_2O_3 with twist ratio, *H/D* of 10 and water in plain tube to be compared are shown in the figure. Through the figure, nanofluid have greater value of Nusselt number than water in plain tube in range of Reynolds number of 2000 and 20000.

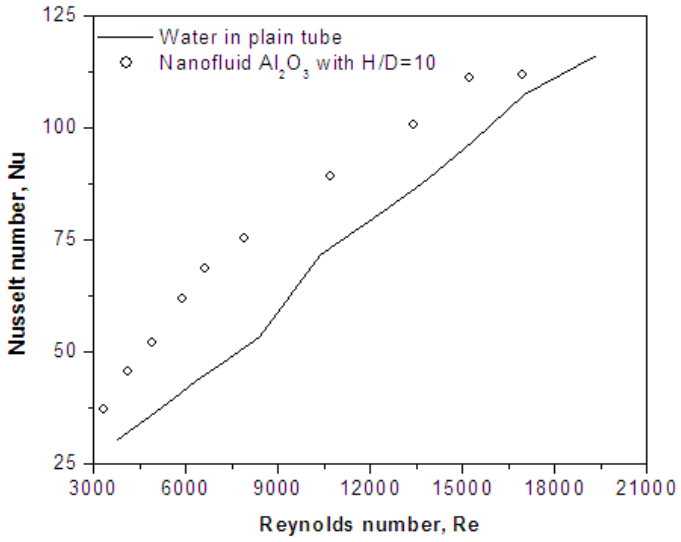

Figure 4.12: Nusselt number versus Reynolds number for nanofluid with *H/D* = 10

4.4.3 For Al_2O_3 with Volume concentration, ϕ = 0.5%; Twist ratio, *H/D* = 15;

Next twist ratio to be tested is 15. The experimental result obtained using nanofluid as working fluid with twist ratio of 15 is provided in Table 4.10. V_{avg} is obtained from totalizer readings, Bulk temperature and average wall temperature are calculated using Eq. 3.5 and 3.6.

Table 4.10: Temperature distribution for Al_2O_3 with Volume concentration, ϕ = 0.5%; Twist ratio, *H/D* = 15;

No.	V_{avg} (Liter/sec)	T_{bulk} (˚C)	`T_{wall} (˚C)
1	0.16	39.9	71.2
2	0.21	38.5	69.4
3	0.25	37.6	68.1
4	0.30	36.5	65.4
5	0.34	35.6	63.7
6	0.40	35.0	61.2
7	0.55	37.8	62.0
8	0.68	37.1	59.7
9	0.75	36.7	57.8
10	0.90	35.6	55.6
11	0.96	33.3	52.5
12	1.09	31.5	50.1

Table 4.11 showing the calculation distribution of mass flow rate, $\dot{m}$, Darcy friction factor, *f*, Prandtl number, *Pr*, Reynolds number, *Re* and heat transfer coefficient, *h*. Nusselt number for experiment is calculated using the experimental data as in subchapter, 3.10.3. The calculation is done for nanofluid of Al_2O_3 with volume concentration of 0.5% and twist ratio of 15.

Table 4.11: Data distribution of experiment for Al_2O_3 with Volume concentration, ϕ = 0.5%; Twist ratio, *H/D* = 15;

V = 190V ; I = 3 A `						
No.	$\dot{m}$	V_{avg}	***Re***	***h***	$Nu_{w,theory}$	$Nu_{w,exp}$
1	0.03647	0.16	3231.7	1099.08	31.18	29.83
2	0.04644	0.21	3997.3	1270.85	36.49	34.78
3	0.05640	0.25	4763.1	1344.47	39.42	36.99
4	0.06632	0.30	5470.4	1646.69	47.17	45.60
5	0.07636	0.34	6169.8	1766.43	50.59	49.19
6	0.08966	0.40	7157.6	2040.33	58.36	57.00
7	0.12275	0.55	10399.7	2322.68	57.59	63.84
8	0.15263	0.68	12739.6	2592.71	69.46	71.56
9	0.16929	0.75	14009.2	2933.57	80.6	81.16
10	0.20258	0.90	16386.3	3042.59	87.19	84.70
11	0.21588	0.96	16575.4	3398.24	104.08	95.95
12	0.24585	1.09	18141.3	3682.57	119.32	105.10

For nanofluid of Al_2O_3 flow in a tube with twist ratio, *H/D* of 15, Experimental Nusselt number is presented in Figure 4.13. The figure shows increasing value of Nusselt number for nanofluid Al_2O_3 with twist ratio, *H/D* of 15 and water in plain tube to be compared. In low range of Reynolds number, Re, nanofluid have greater value of Nusselt number than water in plain tube. After Reynolds number of 10000, water in plain tube have greater value of nanofluid. This due to unstable flow and the flow are not cooled down enough. The pattern of figure similarly as figure for nanofluid for twist ratio of 5.

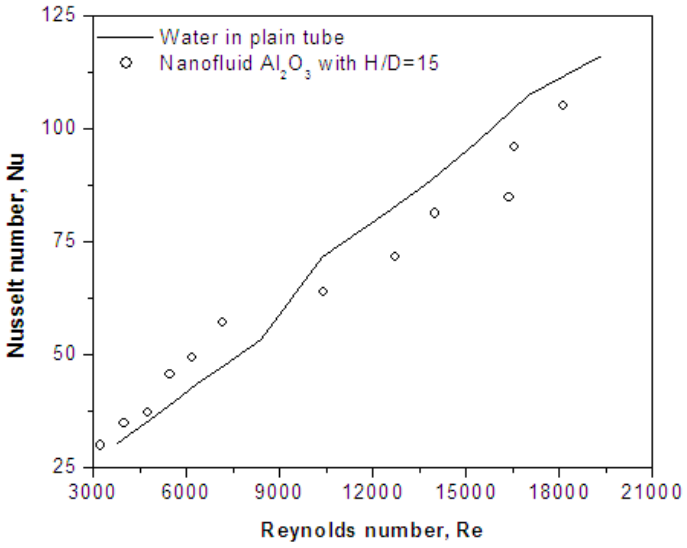

Figure 4.13: Nusselt number versus Reynolds number for nanofluid with *H/D* = 15

4.4.4 For Al_2O_3 with Volume concentration, ϕ = 0.5%; Twist ratio, *H/D* = 83;

Lastly, experimental result obtained using nanofluid as working fluid with twist ratio for 83 is provided in Table 4.10. V_{avg} is obtained from totalizer readings, Bulk temperature and average wall temperature are calculated using Eq. 3.5 and 3.6.

Table 4.12: Temperature distribution for Al_2O_3 with Volume concentration, ϕ = 0.5%; Twist ratio, *H/D* = 83;

No.	V_{avg} (Liter/sec)	T_{bulk} (˚C)	`T_{wall} (˚C)
1	0.16	39.9	72.1
2	0.21	38.5	70.2
3	0.25	37.5	68.7
4	0.30	36.5	66.1
5	0.35	35.5	64.5
6	0.41	35.0	62.1
7	0.55	37.7	62.6
8	0.70	37.0	59.9
9	0.74	36.6	57.3
10	0.86	35.7	55.8
11	0.96	33.3	57.7
12	1.09	31.6	50.3

Table 4.13 showing the calculation distribution of mass flow rate, $\dot{m}$, Darcy friction factor, *f*, Prandtl number, *Pr*, Reynolds number, *Re* and heat transfer coefficient, *h*. Nusselt number for experiment is calculated using the experimental data where have been discussed in previous subchapter, 3.10.3. The calculation is done for nanofluid of Al_2O_3 with volume concentration of 0.5% and twist ratio of 83.

Table 4.13: Data distribution of experiment for Al_2O_3 with Volume concentration, ϕ = 0.5%; Twist ratio, *H/D* = 83;

V = 190V ; I = 3 A `						
No.	$\dot{m}$	V_{avg}	***Re***	***h***	$Nu_{w,theory}$	$Nu_{w,exp}$
1	0.03647	0.16	3228.4	1062.58	31.02	28.85
2	0.04644	0.21	3993.1	1217.51	35.92	33.33
3	0.05635	0.25	4749.0	1326.35	39.73	36.51
4	0.06633	0.30	5465.0	1384.04	40.62	38.33
5	0.07969	0.35	6431.9	1707.96	50.39	47.57
6	0.09298	0.41	7414.4	1979.33	58.58	55.32
7	0.12275	0.55	10388.6	2289.01	58.28	62.93
8	0.15624	0.70	13026.9	2669.24	72.3	73.69
9	0.16597	0.74	13719.5	3091.42	83.25	85.55
10	0.19254	0.86	15591.4	3139.70	90.83	87.38
11	0.21587	0.96	16593.3	2744.57	106.77	77.47
12	0.24588	1.09	18164.3	3469.68	113.51	98.99

Experimental Nusselt number for nanofluid of Al_2O_3 flow in a tube with twist ratio, *H/D* of 83 is presented in Figure 4.14. The figure shows increasing value of Nusselt number for nanofluid Al_2O_3 with twist ratio, H/D of 5 and water in plain tube to be compared. Nanofluid have greater value of Nusselt number than water in plain tube in low range of Reynolds number, Re. After Reynolds number of 8000, water in plain tube has greater value of nanofluid. This due to unstable flow and the flow are not cooled down enough.

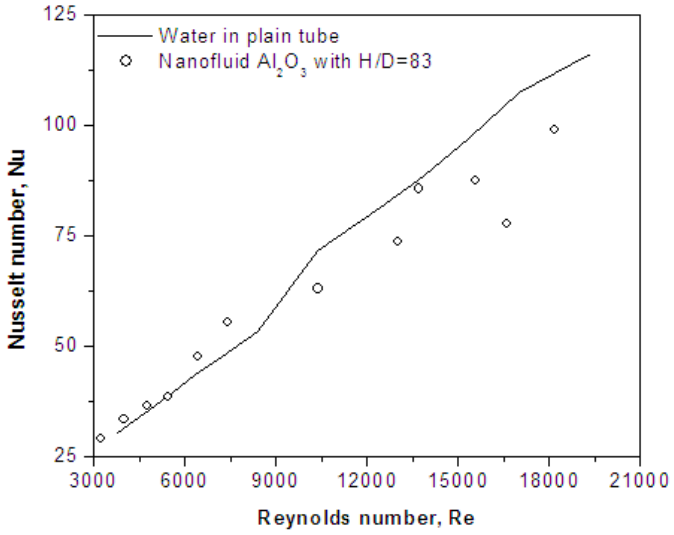

Figure 4.14: Nusselt number versus Reynolds number for nanofluid with *H/D* = 83

4.5 RESULT DISCUSSION

Based on the plotted graph in Figure 4.11 to 4.15, water with *H/D* of 5 have higher Nusselt number than nanofluid Al_2O_3 with *H/D* of 83. Considering the effect of twisted ratio, *H/D*, the turbulent intensity and the flow length obtained from lower twist ratio is higher than those at higher ones. Thus, it can be concluded that by using low twist ratio, Nusselt number is increasing. Besides that, twisted tape in a tube does help increases the enhancement of heat transfer coefficient.

The initial experiment using water as working fluid are plotted using actual values for water in plain tube and in tube with inserted tape. Figure 4.15 shows the comparison between them where using twist ratio of 5 have higher Nusselt number than using twist ratio of 10, 15 and 83. In low range of Reynolds number, Re, water with twisted tapes have greater value of Nusselt number than water in plain tube. After Reynolds number of 10000, water in plain tube have greater value of nanofluid. This due to unstable flow and the flow are not cooled down enough. The condition of environment disturbance need more care.

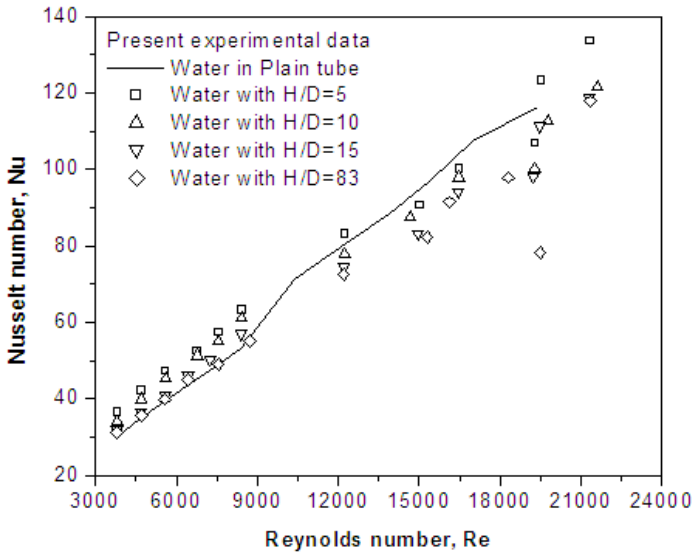

Figure 4.15: Comparison of experimental data of water different twisted ratio with water in plain tube

By using nanofluid Al_2O_3 as the working fluid with different twisted tape, dimensionless parameter, Nusselt number is increase as shown in Figure 4.16. Increasing Nusselt number affected the heat transfer coefficient which means enhance heat transfer rates. High value of Nusselt number influence HTC as in Eq. 2.22, Nusselt number is directionally proportional to HTC.

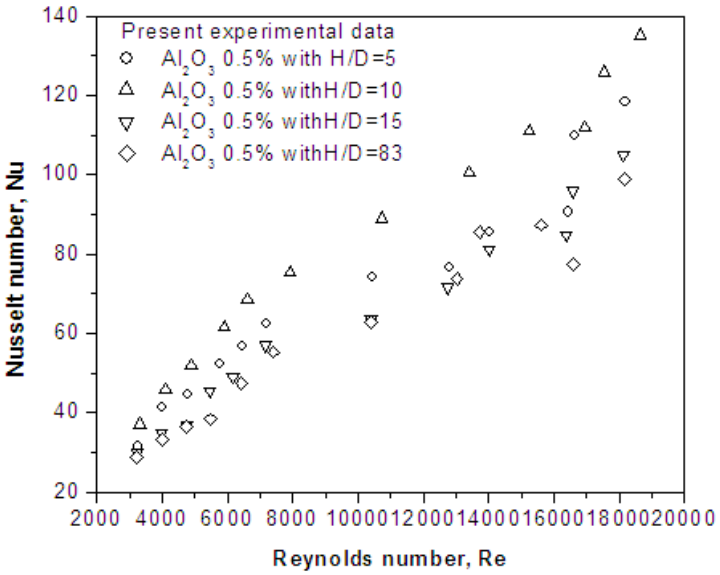

Figure 4.16: Comparison between nanofluid Al_20_3 with different twist ratio, H/D

Comparison between nanofluid Al_2O_3 at different twist ratio, H/D and water in plain tube is presented in Figure 4.17. From the figure it can be observed that higher heat transfer rates are obtained with twisted tape compared to water flow in a plain tube. Nanofluid with twisted tape have greater value of Nusselt number than water in plain tube in low range of Reynolds number, Re. The highest Nusselt number is nanofluid for Alumina with twist ratio of 10 which differ than theory. The highest Nusselt number should be nanofluid Al_2O_3 with twist ratio of 5. This occur due to unstable flow and the flow are not cooled down enough during experiment with twist ratio of 5. Hence, it is recommended that the flow is ensured to be cooled down efficiently

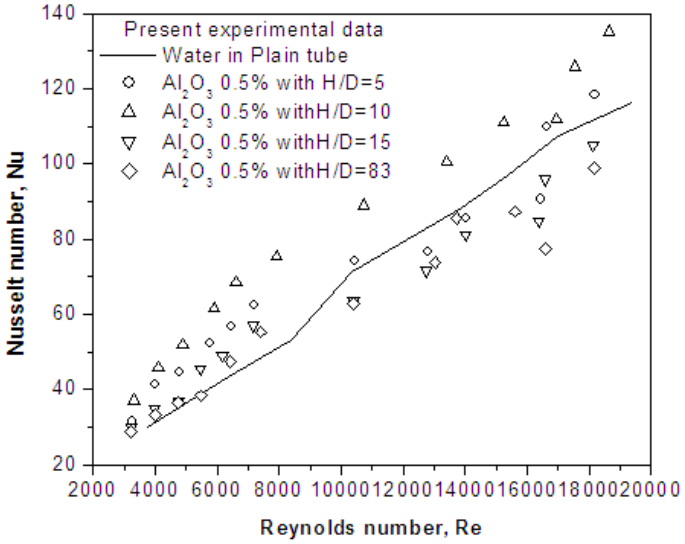

Figure 4.17: Comparison between nanofluid Al_20_3 for different twist ratio, H/D and Water in plain tube

Experiments with twisted tape inserts are conducted with water and nanofluid following the procedure explained earlier for flow in a tube. The procedure is repeated with tapes of different twist ratios of 5, 10, 15 and 83. From Figure 4.18, it can be observed that higher heat transfer rates are obtained with twisted tape inserts compared to nanofluid flow in a tube.

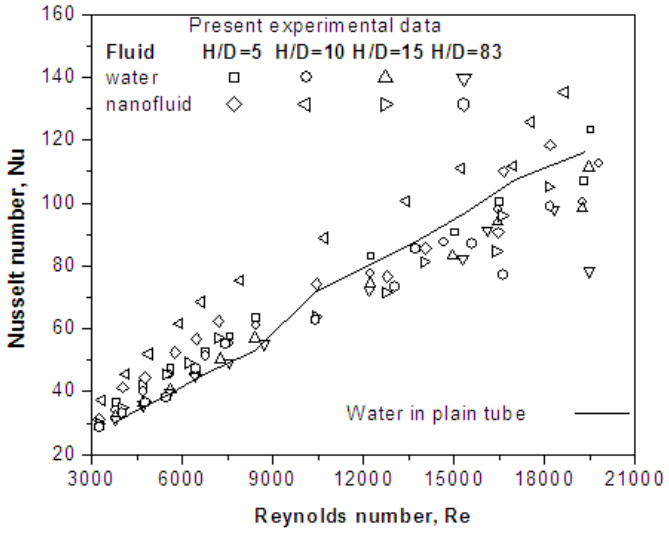

Figure 4.18: Comparison of Nusselt number of water and nanofluid in a tube and with tape inserts.

A comparison of Nusselt number's values versus average velocity of water and nanofluid in a tube and with tape inserts was plotted in Figure 4.19. It is shown that by using nanofluid with higher average velocity in tube of lower twist ratio provides greater heat transfer rate. Highest value of Nusselt number is by using nanofluid Al_2O_3 with twisted tape of 10 between range of average velocity of 0 until 1.4 m/s. Theoretically, twist ratio of 5 should enhance heat transfer of nanofluid greater. However, the disturbance from environment and less efficient chillers should be took care before proceed with experiments. Further recommendation is discussed in Chapter 5.

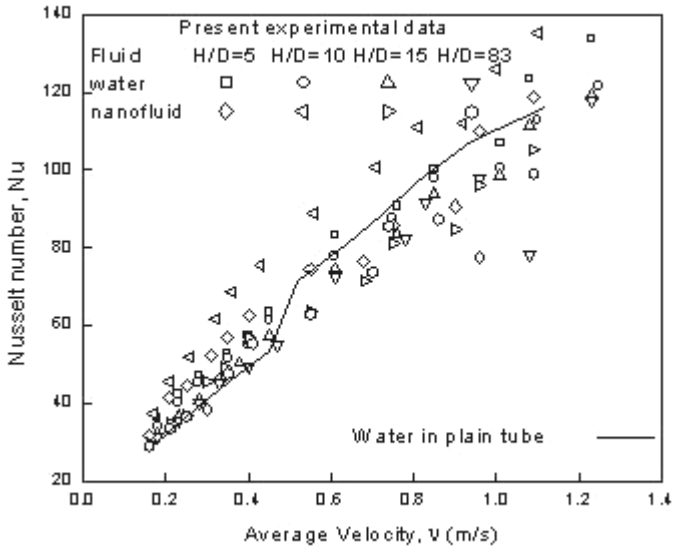

Figure 4.19: Comparison of Nusselt number versus Average Velocity of water and nanofluid in a tube and with tape inserts.

Comparison of the estimation of Nusselt number using Gnielinski (1976) for flow of single phase fluids like water in plain tube, Nusselt number using regression equation develop by Sarma et. al. (2009) for nanofluid of 0.5% in plain tube and present experimental data are presented in Figure 4.16. For regression equation of nanofluid in plain tube is calculated using Eq. 2.23 by assuming *H/D* is 0. From Figure 4.20 it can be observed that higher Nusselt number are obtained with nanofluid in twisted tape inserts compared to nanofluid flow and water in plain tube. Heat transfer coefficients at

Reynolds number of 10,000 and 22,000 with nanofluid of 0.5% volume concentration for twist ratio of 10 is higher when compared to nanofluid and water in a plain tube by 9.07% and 26.71% respectively. Hence, from the relationship between Nusselt number and HTC, as Nusselt number increases, HTC is also increase in directly proportional pattern. Note that Experimental data for comparison of Nusselt number is rarely available in literature for nanofluids with twisted tape insert.

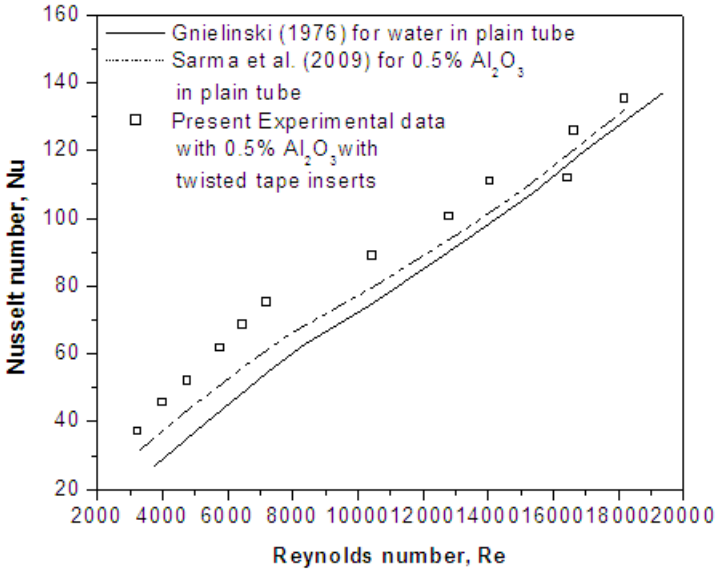

Figure 4.20: Comparison of Nusselt number versus Reynolds number of water and nanofluid in a tube and with tape inserts using Gnielinski (1976), Sarma et al. (2009) and present experimental data.

4.6 CONCLUSION

As conclusion based on the results, nanofluid with twisted tape inserts have higher heat transfer rates than using water with twisted tape inserts and in plain tube. Tape with low twist ratio gives higher Nusselt number than Tape with higher twist ratio for the enhancement of heat transfer rate. Hence, by obtaining result of increasing Nusselt number, heat transfer coefficient also increases. The objectives of the study have been achieved.

CHAPTER 5

CONCLUSION AND RECOMMENDATIONS

5.1 CONCLUSION

The scientific paper concerns on heat transfer coefficient which related directly to heat transfer rate. Conventionally, water is used as working fluid in process of heat transfer. Hence, the paper investigates on how does nanofluid affected rate of heat transfer additionally using twist tape inserts.

Initially, the calibration process using water proven that the result from the setup has reliability characteristic in order to continue with nanofluid. The mean deviation between measured and correlated values of the Nusselt number is in the order of ±10% in the range of Reynolds numbers from 4000 to 20,000. Therefore, the apparatus is reliable to conduct the experiment.

By using lower ratio of twist, H/D =10 for nanofluid, it provides higher Nusselt number for higher Reynolds number. Theoretically, H/D of 5 for nanofluid should have highest value of Nusselt number. Different result than theory is due to environment distraction. The properties of nanofluid are not constant along the experiment gives effect to the result than previous research paper with understanding that the properties do seriously influence the result.

Referring to experimental results for nanofluid, twist tape inserts does enhance the rate of heat transfer compared to heat transfer in a plain tube by using nanofluid as heat transfer's medium. Answering the second research objective, by using twist insert tape with nanofluid as working fluid, the value of Nusselt number is higher compare to

previous literature of Nusselt number for nanofluid and water in plain tube. Heat transfer coefficients at Reynolds number of 10,000 and 22,000 with nanofluid of 0.5% volume concentration for twist ratio of 10 is higher when compared to nanofluid and water in a plain tube by 9.07% and 26.71% respectively. The effect of twisted tape is increases turbulent characteristic of the flow through the plain tube. Hence, due to directly proportionality characteristic in equation of Nusselt number, this result ensuring that heat transfer coefficient also increasing.

The paper reach conclusion as increasing pattern of heat transfer coefficient is achieve by using nanofluid as the working fluid in a tube with inserted tape. Increasing ratio of twist tape causing Nusselt number decrease for nanofluid due to effect of twist tape and varies properties which influence the research study.

5.2 RECOMMENDATIONS

In order to produce more accurate result during this study, some parts need to have more attention and recommendations changes during the study and effective experiment.

The most crucial in this study is nanofluid itself. The process of producing nanofluid does influence the experiment. The researcher must understand clearly on the step by steps. This to ensure that there is no defect in the working fluid.

The apparatus in this study also must have the same concern. Since this experiment relies on thermocouples' reading, hence, the thermocouple must have high sensitivity and read at the suitable point. Thermocouple should have two decimal points and must not miss any mark point that need to be measured.

The different twist ratio of tape insert gives different effect towards heat transfer coefficient. Hence, the inserted tape should be carefully twisted in laboratory. Further research on using other material despite of using aluminum tape for twisted tape is an interesting study.

Through this study, high Reynolds number is the interested region. The parameter can be control based on the flow of working fluid. Therefore, the researcher must know how to control the flow since it is clearly understand that Reynolds number related to the graph's pattern.

Last but not least, the analysis depends on the properties of working fluid. Hence, method on how to calculate or measured the properties must be well chosen. By carefully concern with each aspect for the experiment, it helps the researcher to conduct the experiment.

REFERENCES

Azmi, W. H., Sharma, K.V., Sarma P.K., and Mamat, R. 2010. Influence of Certain Thermo-Physical Properties on Prandtl Number of Water Based Nanofluids, National Conference in Mechanical Engineering Research and Postgraduate Students, FKM Conference Hall, UMP, Kuantan, Pahang, Malaysia; pp. 502-515.

Cengel, Y. A. 2006. *Heat and Mass Transfer: A Practical Approach (3rd ed) SI units*. New York: McGraw-Hill.

Chon, C.H., Kihm, K.D., Lee, S.P., and Choi, S.U.S. 2005. Empirical correlation finding the role of temperature and particle size for nanofluid (Al_2O_3) thermal conductivity enhancement. *Applied physics Letters* **87**: 1-3.

Chopkar, M., Das, P. K. and Manna, I. 2006. Synthesis and characterization of nanofluid for advanced heat transfer applications. *Scr. Mater*. **55**: 549–552.

Das, S. K., Putra, N., Theisen, P., and Roetzel, W. 2003. Temperature dependence of thermal conductivity enhancement for nanofluid. *Journal of Heat Transfer* **125**: 567–574.

Das, S.K., Choi, S.U.S., Yu, W., and Pradeep, T. 2008. *Nanofluids: Science and Technology*. New York: John Wiley & Son, Inc.

Dittus, F. W. and Boelter, L. M. K. 1930. University of California Publications on Engineering 2, p. 433

Duncan, M. A., and D. H. Rouvray. 1989. Microclusters. *Sci. Am.* Dec., 110–115

Eastman, J. A., Choi, S. U. S., Li, S., Thompson, L. J. and Lee, S. 1997. Enhancement thermal conductivity through the development of nanofluids. *Fall meeting of the Materials Research Society (MRS)*, Boston, USA.

Eiamsa-ard, S. 2009. Convective heat transfer in a circular tube with short-length twisted tape insert. *International Communications in Heat and Mass Transfer*. 365–371.

Fotukian, S. M. and Esfahany, M. N. 2010. Experimental investigation of turbulent convective heat transfer od dilute Al_2O_3/Water nanofluid inside circular tube. *International Journal of Heat and Fluid Flow*. **31**: 606-612.

Gnielinski, V. 1976. New Equation for Heat and Mass Transfer in Turbulent pipe and Channel Flow. *International Chemical Engineering*. **19**: 359-368.

Hwang, Y. and Lee. J. 2007. Stability and thermal conductivity characteristics of nanofluids. *Thermochimica Acta*. **30**: 70–74.

Incropera, F. P. 2007. *Fundamentals of Heat and Mass Transfer, Sixth Edition.* Asia: John Wiley & Sons.

Kakaç, S. and Pramuanjaroenkij. A. 2009. Review of convective heat transfer enhancement with nanofluids. *International Journal of Heat and Mass Transfer*. **52**: 3187–3196.

Lopina, R.F. and Bergles, A.E. 1969. Heat transfer and pressure drop in tape-generated swirl flow of single phase water. *Journal Heat Transfer*. **91:** 434–442.

Manglik, R.M. and Bergles, A.E. 1993. Heat transfer and pressure drop correlations for twisted-tape inserts in isothermal tubes: part II – transition and turbulent flows. *Journal Heat Transfer.* **115**: 890–896.

Mansour, R. B., Galanis, N., and Nguyen, C. T. 2007. Effect of uncertainties in physical properties on forced convection heat transfer with nanofluids. *Applied Thermal Engineering.* **27**(1): 240-9.

Masuda, H., Ebata, A., Teramae, K. and Hishinuma, N. 1993. Alteration of thermal conductivity and viscosity of liquid by dispersing ultra fine particles. *Netsu Bussei*. **4**(4): 227–233.

Maxwell, J.C. 1873. *Treatise on electricity and magnetism*. Oxford: Clarendon Press.

Murshed, S.M.S., Leong, K.C. and Yang, C. 2008. Investigations of thermal conductivity and viscosity of nanofluids. *International Journal of Thermal Sciences.* **47**: 560-568.

Pak, B. C. and Cho, I.Y. 1998. Hydrodynamic and heat transfer study of dispersed fluids with sub-micron metallic oxide particles. *Experimental Heat Transfer*. **11**: 151-70.

Sarma, P.K., Subramanyam, T., Kishore, P.S., Rao, V. D. and Kakaç, S. 2003. Laminar convective heat transfer with twisted tape inserts in a tube. *Int. J. Therm. Sci.* **42**: 821–828.

Sarma, P.K., Subramanyam, T., Kishore, P.S., Rao, V. D., Kakaç, S. 2002. A new method to redict convective heat transfer in a tube with twisted tape inserts for turbulent flow. *Int. J. Therm. Sci*. **41**: 955–960.

Smithberg, E. and Landis, F. 1964. Friction and forced convective heat transfer characteristics in tube with twisted-tape swirl generators. *Journal Heat Transfer*. **86**: 39–49.

Sobhan, C. B. and Peterson, G. P. 2008. *Microscale and Nanoscale Heat Transfer: Fundamental and Engineering Application.* United States of America: Taylor & Francis Group.

Sundar, L. S. and Sharma, K.V. 2009. Estimation of heat transfer coefficient and friction factor in the transition flow with low volume concentration of Al_2O_3 nanofluid flowing in a circular tube and with twisted tape insert. *International Communications in Heat and Mass Transfer.* **36**: 503–507.

Sundar, L.S and Sharma, K. V. 2007. Experimental investigation of Heat Transfer Enhancements with Al_2O_3 Nanofluid and Twisted Tape Insert in a Circular Tube. *International Journal of Nanotechnology and Applications*. **25**: 21–28.

Sundar, L.S and Sharma, K. V. 2010. Turbulent heat transfer and friction factor of Al_2O_3 Nanofluid in circular tube with twisted tape inserts. *International Journal of Heat and Mass Transfer*. **53**: 1409-1416.

Taufiq, M. 2010. *Development of the Regression Equation for Specific Heat and Density of Nanofluid.* Bach. degree. Final Year Project. Universiti Malaysia Pahang, Malaysia.

Wang, X., Xu, X. and Choi, S. U. S. 1999. Thermal conductivity of nanoparticle-fluid mixture. *Journal of Thermophysics and Heat Transfer.* **13**(4): 474-480.

Xuan, Y., and Li, Q. 2003. Investigation on convective heat transfer and flow features of nanofluids. *Journal of Heat Transfer*. **125**: 151–155.

Yulong D. and H. C. 2007. Forced convective heat transfer of nanofluids. *VSP and Society of Powder Technology*. **44**: 813–824.

APPENDIX A1

GANTT CHART

No	Task	January				February				March				April			
		W1	W2	W3	W4	W5	W6	W7	W8	W9	W10	W11	W12	W13	W14	W15	W16
1	Searching infromation related with title as basic knowledge																
2	Confirming title of psm with supervisor																
3	Find materials and journals for better understanding																
4	Draft proposal with own ideas																
5	Finalize objectives and scopes																
6	Preparation of Introduction																
7	Preparaton of Literature Review																
8	Discussion and preparation for Methodology																
9	Finalized Project proposal																
10	Prepare slide and technical report for presentation																
11	Submit final report and logbook																
12	Presentation for PSM 1																

Figure 6.1: Gantt chart for FYP 1.

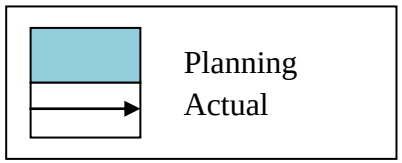

APPENDIX A2

GANTT CHART

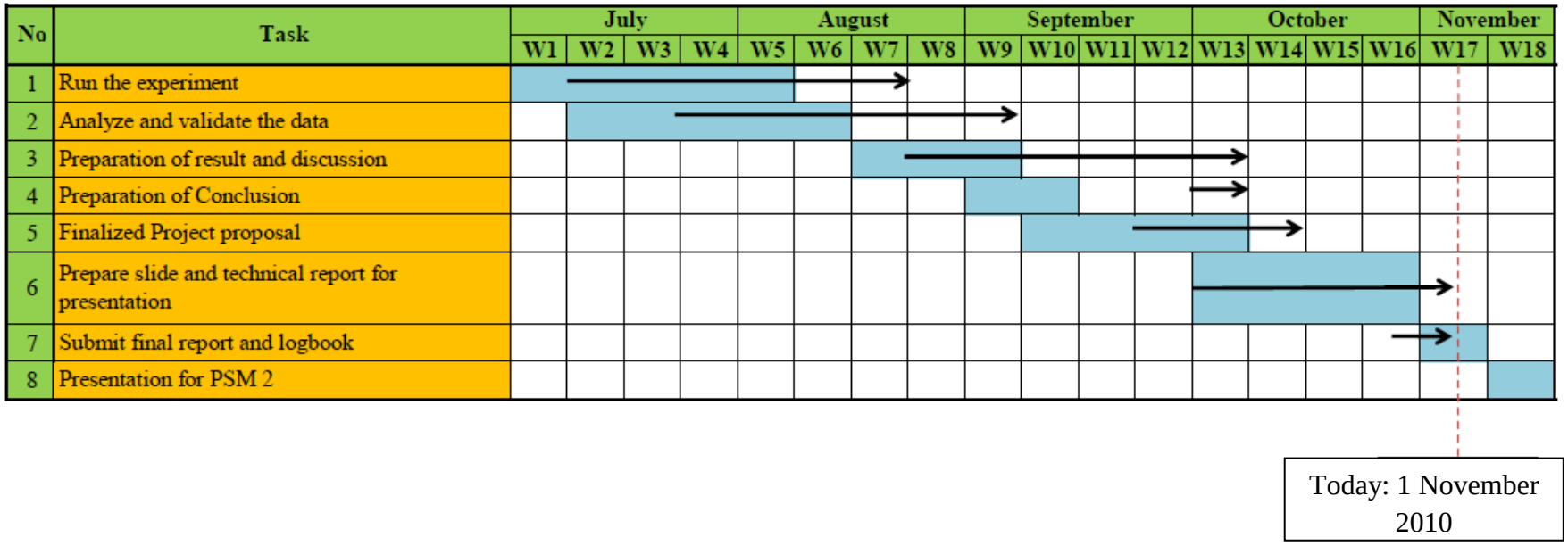

Figure 6.2: Gantt chart for FYP 2.

APPENDIX B

TABLE OF SATURATED WATER PROPERTIES

TABLE A–9

Properties of saturated water

Temp. T, °C	Saturation Pressure P_{sat}, kPa	Density ρ, kg/m³ Liquid	Density ρ, kg/m³ Vapor	Enthalpy of Vaporization h_{fg}, kJ/kg	Specific Heat c_p, J/kg · K Liquid	Specific Heat c_p, J/kg · K Vapor	Thermal Conductivity k, W/m · K Liquid	Thermal Conductivity k, W/m · K Vapor	Dynamic Viscosity μ, kg/m · s Liquid	Dynamic Viscosity μ, kg/m · s Vapor	Prandtl Number Pr Liquid	Prandtl Number Pr Vapor	Volume Expansion Coefficient β, 1/K Liquid
0.01	0.6113	999.8	0.0048	2501	4217	1854	0.561	0.0171	1.792×10^{-3}	0.922×10^{-5}	13.5	1.00	-0.068×10^{-3}
5	0.8721	999.9	0.0068	2490	4205	1857	0.571	0.0173	1.519×10^{-3}	0.934×10^{-5}	11.2	1.00	0.015×10^{-3}
10	1.2276	999.7	0.0094	2478	4194	1862	0.580	0.0176	1.307×10^{-3}	0.946×10^{-5}	9.45	1.00	0.733×10^{-3}
15	1.7051	999.1	0.0128	2466	4185	1863	0.589	0.0179	1.138×10^{-3}	0.959×10^{-5}	8.09	1.00	0.138×10^{-3}
20	2.339	998.0	0.0173	2454	4182	1867	0.598	0.0182	1.002×10^{-3}	0.973×10^{-5}	7.01	1.00	0.195×10^{-3}
25	3.169	997.0	0.0231	2442	4180	1870	0.607	0.0186	0.891×10^{-3}	0.987×10^{-5}	6.14	1.00	0.247×10^{-3}
30	4.246	996.0	0.0304	2431	4178	1875	0.615	0.0189	0.798×10^{-3}	1.001×10^{-5}	5.42	1.00	0.294×10^{-3}
35	5.628	994.0	0.0397	2419	4178	1880	0.623	0.0192	0.720×10^{-3}	1.016×10^{-5}	4.83	1.00	0.337×10^{-3}
40	7.384	992.1	0.0512	2407	4179	1885	0.631	0.0196	0.653×10^{-3}	1.031×10^{-5}	4.32	1.00	0.377×10^{-3}
45	9.593	990.1	0.0655	2395	4180	1892	0.637	0.0200	0.596×10^{-3}	1.046×10^{-5}	3.91	1.00	0.415×10^{-3}
50	12.35	988.1	0.0831	2383	4181	1900	0.644	0.0204	0.547×10^{-3}	1.062×10^{-5}	3.55	1.00	0.451×10^{-3}
55	15.76	985.2	0.1045	2371	4183	1908	0.649	0.0208	0.504×10^{-3}	1.077×10^{-5}	3.25	1.00	0.484×10^{-3}
60	19.94	983.3	0.1304	2359	4185	1916	0.654	0.0212	0.467×10^{-3}	1.093×10^{-5}	2.99	1.00	0.517×10^{-3}
65	25.03	980.4	0.1614	2346	4187	1926	0.659	0.0216	0.433×10^{-3}	1.110×10^{-5}	2.75	1.00	0.548×10^{-3}
70	31.19	977.5	0.1983	2334	4190	1936	0.663	0.0221	0.404×10^{-3}	1.126×10^{-5}	2.55	1.00	0.578×10^{-3}
75	38.58	974.7	0.2421	2321	4193	1948	0.667	0.0225	0.378×10^{-3}	1.142×10^{-5}	2.38	1.00	0.607×10^{-3}
80	47.39	971.8	0.2935	2309	4197	1962	0.670	0.0230	0.355×10^{-3}	1.159×10^{-5}	2.22	1.00	0.653×10^{-3}
85	57.83	968.1	0.3536	2296	4201	1977	0.673	0.0235	0.333×10^{-3}	1.176×10^{-5}	2.08	1.00	0.670×10^{-3}
90	70.14	965.3	0.4235	2283	4206	1993	0.675	0.0240	0.315×10^{-3}	1.193×10^{-5}	1.96	1.00	0.702×10^{-3}
95	84.55	961.5	0.5045	2270	4212	2010	0.677	0.0246	0.297×10^{-3}	1.210×10^{-5}	1.85	1.00	0.716×10^{-3}
100	101.33	957.9	0.5978	2257	4217	2029	0.679	0.0251	0.282×10^{-3}	1.227×10^{-5}	1.75	1.00	0.750×10^{-3}
110	143.27	950.6	0.8263	2230	4229	2071	0.682	0.0262	0.255×10^{-3}	1.261×10^{-5}	1.58	1.00	0.798×10^{-3}
120	198.53	943.4	1.121	2203	4244	2120	0.683	0.0275	0.232×10^{-3}	1.296×10^{-5}	1.44	1.00	0.858×10^{-3}
130	270.1	934.6	1.496	2174	4263	2177	0.684	0.0288	0.213×10^{-3}	1.330×10^{-5}	1.33	1.01	0.913×10^{-3}
140	361.3	921.7	1.965	2145	4286	2244	0.683	0.0301	0.197×10^{-3}	1.365×10^{-5}	1.24	1.02	0.970×10^{-3}
150	475.8	916.6	2.546	2114	4311	2314	0.682	0.0316	0.183×10^{-3}	1.399×10^{-5}	1.16	1.02	1.025×10^{-3}
160	617.8	907.4	3.256	2083	4340	2420	0.680	0.0331	0.170×10^{-3}	1.434×10^{-5}	1.09	1.05	1.145×10^{-3}
170	791.7	897.7	4.119	2050	4370	2490	0.677	0.0347	0.160×10^{-3}	1.468×10^{-5}	1.03	1.05	1.178×10^{-3}
180	1,002.1	887.3	5.153	2015	4410	2590	0.673	0.0364	0.150×10^{-3}	1.502×10^{-5}	0.983	1.07	1.210×10^{-3}
190	1,254.4	876.4	6.388	1979	4460	2710	0.669	0.0382	0.142×10^{-3}	1.537×10^{-5}	0.947	1.09	1.280×10^{-3}
200	1,553.8	864.3	7.852	1941	4500	2840	0.663	0.0401	0.134×10^{-3}	1.571×10^{-5}	0.910	1.11	1.350×10^{-3}
220	2,318	840.3	11.60	1859	4610	3110	0.650	0.0442	0.122×10^{-3}	1.641×10^{-5}	0.865	1.15	1.520×10^{-3}
240	3,344	813.7	16.73	1767	4760	3520	0.632	0.0487	0.111×10^{-3}	1.712×10^{-5}	0.836	1.24	1.720×10^{-3}
260	4,688	783.7	23.69	1663	4970	4070	0.609	0.0540	0.102×10^{-3}	1.788×10^{-5}	0.832	1.35	2.000×10^{-3}
280	6,412	750.8	33.15	1544	5280	4835	0.581	0.0605	0.094×10^{-3}	1.870×10^{-5}	0.854	1.49	2.380×10^{-3}
300	8,581	713.8	46.15	1405	5750	5980	0.548	0.0695	0.086×10^{-3}	1.965×10^{-5}	0.902	1.69	2.950×10^{-3}
320	11,274	667.1	64.57	1239	6540	7900	0.509	0.0836	0.078×10^{-3}	2.084×10^{-5}	1.00	1.97	
340	14,586	610.5	92.62	1028	8240	11,870	0.469	0.110	0.070×10^{-3}	2.255×10^{-5}	1.23	2.43	
360	18,651	528.3	144.0	720	14,690	25,800	0.427	0.178	0.060×10^{-3}	2.571×10^{-5}	2.06	3.73	
374.14	22,090	317.0	317.0	0	—	—	—	—	0.043×10^{-3}	4.313×10^{-5}			

Note 1: Kinematic viscosity ν and thermal diffusivity α can be calculated from their definitions, $\nu = \mu/\rho$ and $\alpha = k/\rho c_p = \nu/\text{Pr}$. The temperatures 0.01°C, 100°C, and 374.14°C are the triple-, boiling-, and critical-point temperatures of water, respectively. The properties listed above (except the vapor density) can be used at any pressure with negligible error except at temperatures near the critical-point value.

Note 2: The unit kJ/kg · °C for specific heat is equivalent to kJ/kg · K, and the unit W/m · °C for thermal conductivity is equivalent to W/m · K.

Source: Viscosity and thermal conductivity data are from J. V. Sengers and J. T. R. Watson, *Journal of Physical and Chemical Reference Data* 15 (1986), pp. 1291–1322. Other data are obtained from various sources or calculated.

APPENDIX C

SAMPLE OF CALCULATION

Sample calculation of heat transfer coefficient, *h* and Nusselt number, *Nu* for water and nanofluid, Al_2O_3 with ϕ=0.5%;

(a) Water

i. Heat Transfer Coefficient and Nusselt number using Ginelski equation, Eq. 2.15.

- Reynolds number, *Re* from Eq. 3.1,

$$Re = \frac{4\dot{m}}{\pi D_i \mu}$$

$$= \frac{4(0.03647 \frac{kg}{s})}{\pi (0.019m)(0.000645 \frac{kg}{m.s})}$$

$$= 3779.4$$

- Prandtl number, *Pr* from Eq. 2.21,

$$Pr = \frac{\nu}{\alpha} = \frac{\mu C_p}{k}$$

$$= \frac{0.000647 \frac{kg}{m.s} \times 4178.3 \frac{J}{kg.K}}{0.6298 \frac{W}{m.K}}$$

$$= 4.2899$$

- Friction Factor, f from Eq. 2.16,

$$\begin{aligned} f &= (1.58 \ln Re - 3.82)^{-2} \\ &= (1.58 \times \ln 3787.93 - 3.82)^{-2} \\ &= 0.0118 \end{aligned}$$

- Nusselt number,Nu from Eq. 2.15,

$$\begin{aligned} Nu &= \frac{\left(\frac{f}{2}\right)(Re - 1000)Pr}{1 + 12.7\left(\frac{f}{2}\right)^{0.5}\left(Pr^{\frac{2}{3}} - 1\right)} \\ &= \frac{\frac{0.0118}{2}(3787.93 - 1000)(4.2802)}{1 + 12.7\left(\frac{0.0118}{2}\right)^{0.5}\left(4.2802^{\frac{2}{3}} - 1\right)} \\ &= 27.15 \end{aligned}$$

- Heat Transfer coefficient, h obtained from Eq. 2.22,

$$\begin{aligned} h &= \frac{Nu.k}{D} \\ &= \frac{27.15 \times 0.6298 \frac{W}{m.K}}{0.019m} \\ &= 899.95 \frac{W}{m^2.K} \end{aligned}$$

ii. Heat Transfer Coefficient and Nusselt number using Dittus-boelter equation, Eq. 2.13.

- Reynolds number, *Re* from Eq. 3.1,

$$Re = \frac{4\dot{m}}{\pi D_i \mu}$$
$$= \frac{4(0.03647\frac{kg}{s})}{\pi(0.019m)(0.000645\frac{kg}{m.s})}$$
$$= 3779.4$$

- Prandtl number, *Pr* from Eq. 2.21,

$$Pr = \frac{\nu}{\alpha} = \frac{\mu C_p}{k}$$
$$= \frac{0.000647\frac{kg}{m.s} \times 4178.3\frac{J}{kg.K}}{0.6298\frac{W}{m.K}}$$
$$= 4.2899$$

- Friction Factor, f from Eq. 2.16,

$$f = (1.58 ln\, Re - 3.82)^{-2}$$
$$= (1.58 \ln(3779.4) - 3.82)^{-2}$$
$$= 0.011828$$

- Nusselt number,*Nu* from Eq. 2.14,

$$\begin{aligned} Nu &= 0.023 Re^{0.8} Pr^{n} \\ &= 0.023 \times 3779.4^{0.8} \times 4.3899^{0.4} \\ &= 27.10 \end{aligned}$$

- Heat Transfer coefficient, *h* obtained from Eq. 2.22,

$$\begin{aligned} h &= \frac{Nu.k}{D} \\ &= \frac{27.10 \times 0.6298 \frac{W}{m.K}}{0.019m} \\ &= 898.36 \frac{W}{m^2.K} \end{aligned}$$

iii. Heat Transfer Coefficient and Nusselt number using Experimental Data.
From Table 4.2, T_b = 39.7 ^oC; T_w = 72.96 ^oC; V = 190 Volt; I = 3 A

- Surface area, A_s

$$\begin{aligned} A_s &= \pi DL = \pi (0.019m)(1.5m) \\ &= 0.0895m^2 \end{aligned}$$

- Crude value for Heat transfer coefficient, $h_{w,exp,(crude)}$ and Crude value for Nusselt number, $Nu_{w,exp,(crude)}$ from Eq. 3.2, 3.3, 3.5 and 3.6,

$$\dot{Q}_{\text{supplied}} = \dot{Q}_{\text{absorbed}}$$

$$V \times I = h_{w,exp.\,(Crude)} A_s (T_w - T_b)_{avg}$$

$$h_{w,exp.\,(Crude)} = \frac{V \times I}{A_s (T_w - T_b)_{avg}}$$

$$= \frac{190V \times 3\,Amphere}{0.0895m^2 (72.96 - 39.70)°C}$$

$$= 191.41 \frac{W}{m^2.K}$$

$$Nu_{exp,\,(Crude)} = \frac{h_{w,exp,\,(Crude)} D}{k}$$

$$= \frac{191.41 \frac{W}{m^2.K} (0.019m)}{0.6298 \frac{W}{m.K}}$$

$$= 5.77$$

- Theory value for Heat transfer coefficient, $h_{w,theory}$ and Crude value for Nusselt number, $Nu_{w,exp,(crude)}$

$$\frac{h_{w,\exp(Crude)}}{h_{w,\ theory}} = \frac{Nu_{w,\exp(Crude)}}{Nu_{w,theory}}$$

$$h_{w,theory} = h_{w.\exp(True\,Value)} = h_{w,\exp(Crude)} \times \left(\frac{Nu_{w,theory}}{Nu_{w,\exp(Crude)}} \right)$$

$$= 191.41 \frac{W}{m^2.K} \times \left(\frac{30.17}{5.77} \right)$$

$$= 1000.84 \frac{W}{m^2.K}$$

$$Nu_{exp,new(True\ Value)} = \frac{h_{theory,water} D}{k}$$

$$= \frac{1000.84 \frac{W}{m^2.K}(0.019m)}{0.6298 \frac{W}{m.K}}$$

$$= 30.17$$

(b) Nanofluid Al_2O_3 with ϕ= 0.5% and *H/D*=5;

From Table 4.4.6, T_b = 40.15 ^oC; T_w = 68.73 ^oC; V = 190 Volt; I = 3 A

- Surface area, A_s

$$A_s = \pi DL = \pi(0.019m)(1.5m)$$

$$= 0.0895m^2$$

- Crude value for Heat transfer coefficient, $h_{,w,exp,(crude)}$ from Eq. 3.2, 3.3, 3.5 and 3.6,

$$\dot{Q}_{supplied} = \dot{Q}_{absorbed}$$

$$V \times I = h_{w,exp.(Crude)} A_s (T_w - T_b)_{avg}$$

$$h_{w,exp.(Crude)} = \frac{V \times I}{A_s (T_w - T_b)_{avg}}$$

$$= \frac{190V \times 3\,Amphere}{0.0895m^2(68.73 - 40.15)°C}$$

$$= 222.75 \frac{W}{m^2.K}$$

- Theory value for Heat transfer coefficient, $h_{,w,theory}$ and Crude value for Nusselt number, $Nu_{w,exp,(crude)}$

$$\frac{h_{nf,\exp(Crude)}}{hnf} = \frac{Nu_{w,\exp(Crude)}}{Nu_{w,theory}}$$

$$h_{nf,theory} = h_{nf.\exp(True\,Value)} = h_{nf,\exp(Crude)} \times \left(\frac{Nu_{w,theory}}{Nu_{w,\exp(Crude)}} \right)$$

$$= 222.75 \frac{W}{m^2.K} \times \left(\frac{30.03}{5.77} \right)$$

$$= 1159.30 \frac{W}{m^2.K}$$

Hence,

$$Nu_{exp,new(True\,Value)} = \frac{h_{theory,nf} D}{k}$$

$$= \frac{1159.30 \frac{W}{m^2.K} (0.019m)}{0.7010 \frac{W}{m.K}}$$

$$= 31.42$$